



Combining mitochondrial DNA and morphological data to delineate four new millipede species and provisional assignment to the genus *Apeuthes* Hoffman & Keeton (Diplopoda : Spirobolida : Pachybolidae : Trigoniulinae)

Piyatida Pimvichai^{A,*} , Somsak Panha^B and Thierry Backeljau^{C,D}

For full list of author affiliations and declarations see end of paper

*Correspondence to:

Piyatida Pimvichai
Department of Biology, Faculty of Science,
Mahasarakham University, Maha Sarakham
44150, Thailand
Email: piyatida.p@msu.ac.th

Handling Editor:

Gonzalo Giribet

ABSTRACT

Hitherto, the millipede genus *Apeuthes* (family Pachybolidae, subfamily Trigoniulinae) was only known from three species described in Vietnam based on morphological characters. The present study uses two partial mitochondrial gene fragments (cytochrome c oxidase I (COI) and 16S ribosomal RNA) and morphology to define four new *Apeuthes* species from Malaysia, Thailand and Vietnam: *A. fimbriatus*, sp. nov., *A. longeligulatus*, sp. nov., *A. pollex*, sp. nov. and ?*A. spininavis*, sp. nov. The intraspecific COI sequence divergence of two *Apeuthes* species is 3–7% (mean: 5%) and the interspecific divergence of five species is 11–16% (mean: 13.7%). All members of the genus share unique male characters, viz the posterior gonopod telopodite with several dentate, serrate or tuberculate lamellae in a boat-like cavity or a boat-like cavity covered with spines. The delimitation of the four new species is supported by the congruence between mitochondrial DNA and morphological data. However, while the monophyly of Trigoniulinae is well supported, the relationships within this subfamily, and particularly among *Apeuthes* species, including the monophyly of *Apeuthes*, lack strong support. Therefore assignment of the four new species, and particularly of ?*A. spininavis* sp. nov., to the genus *Apeuthes* is tentative and awaits a comprehensive revision of the group.

Keywords: DNA barcoding, Malaysia, mitochondrial DNA, monotypic genera, phylogeny, species delineation, Thailand, Trigoniulinae, Vietnam.

Introduction

Millipedes (Diplopoda) are a highly diverse group of arthropods with 16 orders, 140 families and more than 14 000 species (Enghoff *et al.* 2015; MilliBase, <https://millibase.org/>, accessed 12 June 2021). One large millipede family is the Pachybolidae Cook, 1897 (order Spirobolida Bollman, 1893), which currently contains ~60 genera and more than 280 described species. Yet, by extrapolation from the recent discovery of numerous new pachybolid species in Madagascar (e.g. Wesener and Enghoff 2009; Wesener *et al.* 2009a, 2009b) and South-east Asia (Pimvichai *et al.* 2018), it is expected that many more pachybolid species still need to be discovered and described. The present study reports on four new species from Malaysia, Thailand and Vietnam ascribed to the poorly defined pachybolid subfamily Trigoniulinae Attems, 1909 (see Hoffman 1962; Enghoff *et al.* 2015). The best known species of this group is the cosmopolitan *Trigoniulus corallinus* (Gervais, 1842), whose genome was recently sequenced (Qu *et al.* 2020). At least five ‘trigoniuline’ genera have been reported from mainland South-east Asia: *Apeuthes* Hoffman & Keeton, 1960, *Decelus* Hoffman & Keeton, 1960, *Eucarlia* Brölemann, 1913, *Leptogoniulus* Silvestri, 1897 and *Trigoniulus* Pocock, 1894. These genera include cylindrical millipedes of ~5–8-cm length with a diameter of ~3.9–5.4 mm. Based on morphology, three of the four new species described in the present study are placed in the genus *Apeuthes*. However, the fourth new species, while overall being quite similar to the

Received: 17 May 2021
Accepted: 30 June 2021
Published: 16 February 2022

Cite this:

Pimvichai P *et al.* (2022)
Invertebrate Systematics
36(2), 91–112. doi:[10.1071/IS21038](https://doi.org/10.1071/IS21038)

© 2022 The Author(s) (or their employer(s)). Published by CSIRO Publishing.
This is an open access article distributed under the Creative Commons Attribution-NonCommercial-NoDerivatives 4.0 International License ([CC BY-NC-ND](https://creativecommons.org/licenses/by-nc-nd/4.0/))

OPEN ACCESS

other three, differs markedly in its posterior gonopod. Therefore, its assignment to *Apeuthes* is less obvious and will need to be verified in the future. In addition to using morphological and DNA sequence data to describe the four new *Apeuthes* species, this study uses these data to address the status and monophyly of the genus *Apeuthes* and the subfamily Trigoniulinae.

Material and methods

Specimens were hand collected in the field (for locality data see Table 1) and subsequently kept in a freezer at -20°C for DNA studies. Some specimens were directly preserved in 70% ethanol for morphological studies. Specimens from the following collections were also examined:

- CUMZ, Museum of Zoology, Chulalongkorn University, Bangkok, Thailand.
- NHMW, Naturhistorisches Museum, Vienna, Austria.
- NHMD, Natural History Museum of Denmark, University of Copenhagen, Denmark.

This research was conducted under the approval of the Animal Care and Use regulations (numbers U1-07304-2560 and IACUC-MSU-037/2020) of the Thai government.

Morphology

Gonopods were photographed with a digital camera manipulated using the program Helicon Remote (ver. 3.1.1.w; HeliconSoft, Kharkiv, Ukraine). Zerene Stacker Pro software was used for image-stacking (Zerene Systems, Richland, WA, USA). Drawings were made using a stereo-microscope and photographs. Samples for scanning electron microscopy (SEM) were air-dried directly from alcohol and sputter-coated for 250 s with gold. SEM micrographs were taken with an environmental scanning electron microscope (ESEM; Quanta 200, FEI, Hillsboro, OR, USA). The identification and classification of the specimens followed Attems (1938), Hoffman and Keeton (1960) and Jeekel (2001). Voucher specimens were deposited in the collection of CUMZ.

DNA extraction, amplification and sequencing

Total genomic DNA was extracted from dissected legs using the NucleoSpin Tissue kit (Macherey-Nagel, Düren, Germany) following the manufacturer's instructions. PCR amplifications and sequencing were done as described by Pimvichai et al. (2020). Seven specimens were sequenced: *Apeuthes maculatus* (Attems, 1938) Am26; *A. fimbriatus*, sp. nov. BMP; *A. longeligulatus*, sp. nov. TPP; *A. pollex*, sp. nov. SMR; *A. pollex*, sp. nov. SML; *A. pollex*, sp. nov. WTS and ?*A. spininavis*, sp. nov. ABB (specimens, codes and locations

are listed in Table 1). The COI fragment was amplified with the primers LCO-1490 and HCO-2198 (Folmer et al. 1994) and the 16S ribosomal RNA (rRNA) fragment was amplified with the primers 16Sar and 16Sbr (Kessing et al. 2004). The COI data included 47 specimens, representing 16 genera and 41 species of ingroup taxa (Table 1). The 16S rRNA data included 43 specimens, i.e. the same specimens as for COI, minus *Atopochetus anaticeps* Pimvichai, Enghoff, Panha & Backeljau, 2018; *Benoitolus birgitae* (Hoffman, 1981); *Coxobolellus simplex* Pimvichai, Enghoff, Panha & Backeljau, 2020; *Trachelomegalus* sp.; *Narceus annularis* Rafinesque, 1820 and *Paraspirobolus lucifugus* (Gervais, 1837), and including *Litostrophus scaber* (Verhoeff, 1938) and *Trachelomegalus* cf. *hoplurus*, representing 13 genera and 37 species of ingroup taxa. The combined COI + 16S rRNA data included 41 specimens representing 12 genera and 35 species of ingroup taxa. Three species of the order Spirostreptida Brandt, 1833, viz *Anurostreptus barthelemyae* Demange, 1961 (Harpagophoridae Attems, 1909); *Chonecambala crassicauda* Mauriès & Enghoff, 1990 (Pericambalidae Silvestri, 1909) and *Thyropygus allevatus* (Karsch, 1881) (Harpagophoridae) were used as outgroup. All new nucleotide sequences have been deposited in GenBank under accession numbers MZ568653–MZ568659 and MZ567159–MZ567165 for the 16S rRNA and COI fragments respectively. Sample data and voucher codes are provided in Table 1.

Sequence alignment and phylogenetic analysis

CodonCode Aligner (ver. 4.0.4, CodonCode Corporation, Centerville, MA, USA) was used to assemble the forward and reverse sequences and to check for errors and ambiguities. The COI and 16S rRNA sequences were checked with the Basic Local Alignment Search Tool (BLAST, National Center for Biotechnology Information, Bethesda, MD, USA) and compared with reference sequences in GenBank. They were aligned using MUSCLE (ver. 3.6, see <https://www.drive5.com/muscle/>; Edgar 2004). The alignments consisted of 660 bp for COI and 458 bp for 16S rRNA (gaps were excluded by complete deletion). The sequences were checked for ambiguous nucleotide sites, saturation and phylogenetic signal using DAMBE (ver. 5.2.65, see <http://dambe.bio.uottawa.ca/DAMBE/dambe.aspx>; Xia 2018). MEGA (ver. X, see <http://www.megasoftware.net>; Kumar et al. 2018) was used to (1) check for stop codons, (2) translate COI protein-coding sequences into amino acids, (3) calculate uncorrected pairwise *p*-distances among sequences, and (4) evaluate transition/transversion ratios.

Phylogenetic trees were constructed using maximum likelihood (ML) and Bayesian inference (BI). The shape parameter of the gamma distribution, based on 16 rate categories, was estimated using ML analysis. ML trees were inferred with RAXML (ver. 8.2.12, see https://www.phylo.org/index.php/tools/raxmlhpc2_tgb.html; Stamatakis 2014) through

Table 1. Specimens from which the *COI* or *16S* rRNA gene fragments were used.

	Voucher code	Locality	COI	16S rRNA
Genus <i>Apeuthes</i>				
<i>A. maculatus</i> Amc	NHMW-Inv. No. 2395	South Annam, VIETNAM	MF187404	MF187360
<i>A. maculatus</i> Am26	NHMD 621697	Nha Trang, Bao Dai Villas Hotel, in garden, VIETNAM	MZ567159	MZ568653
<i>A. fimbriatus</i> , sp. nov. BMP	CUMZ D00144	Bach Ma Peak, Da Nang, VIETNAM	MZ567160	MZ568654
<i>A. longeligulatus</i> , sp. nov. TPP	CUMZ D00140	Tham Phet Po Thong, Klong Hard, Sa Kao, THAILAND	MZ567161	MZ568655
<i>A. pollex</i> , sp. nov. SMR	CUMZ D00141	Sra Morakot, Klongthom, Krabi, THAILAND	MZ567162	MZ568656
<i>A. pollex</i> , sp. nov. SML	CUMZ D00142	Koh 8, Similan islands, Phang-Nga, THAILAND	MZ567163	MZ568657
<i>A. pollex</i> , sp. nov. WTS	CUMZ D00143	Tham Sue Temple, Muang, Krabi, THAILAND	MZ567164	MZ568658
? <i>A. spininavis</i> , sp. nov. ABB	CUMZ D00145	Air Banun, Perak, MALAYSIA	MZ567165	MZ568659
Genus <i>Atopochetus</i>				
<i>A. anaticeps</i> SVL	CUMZ D00091	Srivilai temple, Chalermprakiet, Saraburi, THAILAND	MF187405	–
<i>A. dollfusii</i> DOL	NHM	Cochinchina, VIETNAM	MF187412	MF187367
<i>A. helix</i> SPT	CUMZ D00094	Suan Pa Thong Pha Phum, Kanchanaburi, THAILAND	MF187416	MF187371
<i>A. moulmeinensis</i> TAK	CUMZ D00095	Km 87, Tha Song Yang, Tak, THAILAND	MF187417	MF187372
<i>A. setiferus</i> HPT	CUMZ D00097	Hub Pa Tard, Lan-Sak, Uthaitani, THAILAND	MF187419	MF187374
<i>A. spinimargo</i> Ton27	ZMUC 00047013	Koh Yo, Songkhla, THAILAND	MF187423	MF187377
<i>A. truncatus</i> SML	CUMZ D00101	Koh 8, Similan islands, Phang-Nga, THAILAND	MF187424	MF187378
<i>A. uncinatus</i> KMR	CUMZ D00102	Khao Mar Rong, Bangsapan, Prachuapkhirikhan, THAILAND	MF187425	MF187379
<i>A. weseneri</i> Tos29	ZMUC 00047003	Supar Royal Beach Hotel, Khanom, Nakhonsrithammarat, THAILAND	MF187431	MF187384
Genus <i>Aulacobolus</i>				
<i>A. uncopysus</i> Auc	NHMW-Inv. No.2375	Nilgiris, South India, INDIA	MF187433	MF187386
Genus <i>Benoitolus</i>				
<i>B. birgitae</i> BBG	NHMD 621687	Chiang Dao, Chiang Mai, THAILAND	MT328992	–
Genus <i>Coxobolellus</i>				
<i>C. albiceps</i> Stpw	CUMZ D00121	Tham Pha Tub, Muang District, Nan Province, THAILAND (green individual)	MT328994	MT328211
<i>C. compactogonus</i> SKR	CUMZ D00134	Sakaerat Environmental Research Station, Wang Nam Khiao District, Nakhon Ratchasima Province, THAILAND	MT328998	MT328215
<i>C. fuscus</i> HKK	CUMZ D00133	Kroeng Krawia waterfall, Sangkhla Buri District, Kanchanaburi Province, THAILAND	MT328999	MT328216
<i>C. nodosus</i> SPW	CUMZ D00126	Chao Por Phawo Shrine, Mae Sot District, Tak Province, THAILAND	MT329000	MT328217
<i>C. serratus</i> KKL	CUMZ D00132	Khao Kalok, Pran Buri District, Prachuap Khiri Khan Province, THAILAND	MT329001	MT328218
<i>C. simplex</i> TNP	CUMZ D00136	Tham Pha Pha Ngam, Mae Prik District, Lampang Province, THAILAND	MT329002	–
<i>C. tenebris</i> TPL	CUMZ D00120	Wat Tham Phrom Lok Khao Yai, Sai Yok District, Kanchanaburi Province, THAILAND	MT329004	MT328220
<i>C. tigris</i> TYE	CUMZ D00131	Tham Yai I, Pathio District, Chumphon Province, THAILAND	MT329006	MT328222
<i>C. transversalis</i> Stpg	CUMZ D00125	Tham Pha Tub, Muang District, Nan Province, THAILAND	MT329007	MT328223
<i>C. valvatus</i> BRC	CUMZ D00128	Tham Borichinda, Chom Thong District, Chiang-Mai Province, THAILAND	MT329008	MT328224
Genus <i>Leptogoniulus</i>				

(Continued on next page)

Table 1. (Continued)

	Voucher code	Locality	COI	16S rRNA
<i>L. sorornus</i> BTN	CUMZ D00109	Botanical Garden, Penang, MALAYSIA	MF187434	MF187387
Genus <i>Litostrophus</i>				
<i>L. chamaeleon</i> PPT	CUMZ D00111	Phu Pha terb, Mukdahan, THAILAND	MF187436	MF187389
<i>L. saraburensis</i> PKS	CUMZ D00113	Phukhae Botanical Garden, Saraburi, THAILAND	MF187438	MF187391
<i>L. scaber</i> Sca	ZSM-ZSMA 20051663	Tonkin, VIETNAM	–	MF187392
<i>L. segregatus</i> Ls19	NHMD 621686	Koh Kut, Trad, THAILAND	MF187440	MF187394
Genus <i>Madabolus</i>				
<i>M. maximus</i> Mm4	ZMUC 00047007	de Toliara Province, Parc National de Bermaraha, South Bank of Manambolo River, Near Tombeau Vazimba, MADAGASCAR	MF187441	MF187395
Genus <i>Narceus</i>				
<i>N. annularis</i>			NC_003343.1	–
Genus <i>Parabolus</i>				
<i>P. dimorphus</i> Pd34	ZMUC 00047004	Dar es Salaam, TANZANIA	MF187442	MF187396
Genus <i>Paraspirobolus</i>				
<i>P. lucifugus</i>			AB608779.1	
Genus <i>Pelmatojulus</i>				
<i>P. tigrinus</i> Pt2	ZMUC 00047008	Southern part of the Comoé N.P., 30 km north of Kakpin, CÔTE d'IVOIRE	MF187443	MF187397
<i>P. togoensis</i> Pto6	ZMUC 00047006	Biakpa, GHANA	MF187444	MF187398
Genus <i>Pseudospirobolellus</i>				
<i>Pseudospirobolellus</i> <i>avernus</i> GPG	CUMZ D00117	Gua Pulai, Gua Musang, Kelantan, MALAYSIA	MT329011	MT328226
<i>Pseudospirobolellus</i> sp. KCS	CUMZ D00118	Koh Chuang, Sattahip, Chonburi, THAILAND	MT329012	MT328227
Genus <i>Rhinocricus</i>				
<i>R. parvus</i> Rp49	ZMUC 00047009	Puerto Rico, USA	MF187449	MF187403
Genus <i>Trachelomegalus</i>				
<i>T. sp.</i> Tr54	ZMUC 00047012	Borneo Sabah, MALAYSIA	MF187445	–
<i>T. cf. hoplurus</i> Th	ZMUC 00047002	Borneo Sarawak, Niah, MALAYSIA	–	MF187399
Genus <i>Trigoniulus</i>				
<i>T. corallinus</i> Tco15	ZMUC 00047010	Vientiane, LAOS	MF187446	MF187400
Outgroup				
Genus <i>Anurostreptus</i>				
<i>A. barthelemyae</i> Tlb	CUMZ D00003	Thale-Ban N.P., Khuan-Don, Satun, THAILAND	KC519469	KC519543
Genus <i>Chonecambala</i>				
<i>C. crassicauda</i> Ttp	CUMZ-D00001	Ton-Tong waterfall, Pua, Nan, THAILAND	KC519467	KC519541
Genus <i>Thyropygus</i>				
<i>T. allevatus</i> Bb	CUMZ-D00013	BangBan, Ayutthaya, THAILAND	KC519479	KC519552

Note: names of countries are in capitals. Abbreviations after species names refer to the isolate of each sequence. GenBank accession numbers are indicated for each species; –, no sequences were obtained. CUMZ, Museum of Zoology, Chulalongkorn University, Bangkok, Thailand; NHMD, Natural History Museum of Denmark; NHMW, Naturhistorisches Museum, Vienna, Austria; NHM, The Natural History Museum, London, United Kingdom; ZMUC, Zoological Museum, University of Copenhagen, Copenhagen, Denmark; ZSM, Bavarian State Collection of Zoology, Munich, Germany.

the Cyberinfrastructure for Phylogenetic Research (CIPRES) Science Gateway (Miller *et al.* 2010) using a generalised time reversible (GTR) + gamma (G) substitution model and 1000 bootstrap replicates to assess branch support. The *COI* sequence alignment was partitioned by 1st, 2nd and 3rd codon position and the concatenated sequence alignment was partitioned by gene fragment and by 1st, 2nd and 3rd codon position for the *COI* portion of the concatenated alignment. BI trees were constructed with MrBayes (ver. 3.1.2, see http://www.phylo.org/index.php/tools/mrbayes_xsede.html; Huelsenbeck and Ronquist 2001) for *COI* and 16S rRNA separately, as well as for the combined data. Substitution models were inferred separately for each gene fragment using PartitionFinder 2 on XSEDE (ver. 2.1.1, see http://www.phylo.org/index.php/tools/partitionfinder2_xsede.html; Lanfear *et al.* 2017) through the CIPRES Science Gateway (Miller *et al.* 2010). BI trees were run for 2 million generations (heating parameters were 0.05 for *COI* and 0.07 for 16S rRNA and combined datasets), sampling every 1000 generations. Convergences were confirmed by verifying that the standard deviations of split frequencies were below 0.01. Then the first 1000 trees were discarded as burn-in, so that the final consensus tree was built from the last 3002 trees. Support for nodes was assessed by posterior probabilities.

We consider clades with bootstrap values (BV) of $\geq 70\%$ to be well supported (Hillis and Bull 1993) and $< 70\%$ as poorly supported. For BI analyses, we considered clades with posterior probabilities (PP) of ≥ 0.95 to be well supported (San Mauro and Agorreta 2010) and below as poorly supported.

Species delimitation

Putative species were explored by applying these tools to the *COI* sequence data: Assemble Species by Automatic Partitioning (ASAP) (<https://bioinfo.mnhn.fr/abi/public/asap/asapweb.html>; Puillandre *et al.* 2021); the General Mixed Yule Coalescent (GMYC) method (Fujisawa and Barraclough 2013); and the Poisson Tree Process (PTP) (Zhang *et al.* 2013).

ASAP is a new tool to delineate species based on species partition hypotheses derived from genetic distances between DNA sequences. The data were run with the default settings: split groups below 0.01 probability; keep 10 best scores; use fixed seed value -1 ; and highlights results between the genetic distances 0.005 and 0.05. *COI* sequence divergence was estimated with the K80 (Kimura 1980) substitution model.

GMYC requires the input of an ultrametric tree from BEAST (ver. 1.8.2, see <http://tree.bio.ed.ac.uk/software/beast/>; Drummond *et al.* 2012). An XML file was made with the BEAUti interface (ver. 1.8.2, see <http://www.beast.community/>) under a lognormal relaxed (uncorrelated) molecular clock with the GTR substitution model.

Putative species were identified using the single and multiple GMYC thresholds using the web interface at <https://species.h-its.org/gmyc/>.

The PTP species delimitation method was applied to the RAXML *COI* gene tree using <https://species.h-its.org/ptp/> to identify the most likely classification of branches into population and species-level processes, delimiting evolutionarily significant units (Tang *et al.* 2014).

Results

The nucleotide frequencies in the aligned *COI* gene fragment (660 bp) were: A, 0.282; C, 0.209; G, 0.160; T, 0.349, with a 36.9% GC content. The uncorrected *p*-distance between the sequences ranged from 0.03 to 0.26 (Table 2). The nucleotide frequencies in the aligned 16S rRNA gene fragment (458 bp) were: A, 0.324; C, 0.110; G, 0.212; T, 0.354, with a 32.2% GC content. The uncorrected *p*-distance between the sequences ranged from 0.02 to 0.29 (Table 3). The uncorrected *p*-distance between the sequences from *COI* + 16S rRNA dataset (1118 bp) ranged from 0.03 to 0.26.

Phylogeny

The ML and BI trees based on the separate and combined datasets (*COI*, 16S rRNA and *COI* + 16S rRNA) were largely congruent with respect to the well-supported branches (by visual inspection of the branching pattern). The combined *COI* + 16S rRNA tree is used for further discussion (Fig. 1). The separate *COI* and 16S rRNA trees are presented in Supplementary Fig. S1, S2). PartitionFinder indicated that the best substitution model for BI analysis was GTR + G for all datasets.

The tree based on the combined dataset includes representatives of three Spirobolida families (Pachybolidae, Pseudospirobolellidae Brölemann, 1913 and Rhinocricidae Brölemann, 1913), together forming a well-supported ingroup clade (BV = 88; PP = 1.00), with well-supported subclades for non-trigoniuline Pachybolidae (BV = 80; PP = 1.00), Pseudospirobolellidae (BV = 99; PP = 1.00) and Trigoniulinae (BV = 100; PP = 1.00). This latter clade comprises 10 sequences of 7 species, including *Leptogoniulus sorornus* (Butler, 1876); *Trigoniulus corallinus* (Gervais, 1842); *Apeuthes maculatus*; ?*A. spininavis*, sp. nov.; *A. longeligulatus*, sp. nov.; *A. fimbriatus*, sp. nov., and *A. pollex*, sp. nov. However, the relationships among these seven species and the monophyly of the genus *Apeuthes*, even if ?*A. spininavis*, sp. nov. is excluded, are inconsistently supported.

Species delimitation based on *COI* sequences

GMYC

With both the single and multiple thresholds, the ML values of the null model (= all sequences belong to a single

Table 2. Estimates of cytochrome c oxidase I (*COI*) sequence divergences (uncorrected *p*-distances) within and among Trigoniulinae species and related taxa (rounded to two decimal places).

[illegible]

(Continued on next page)

Table 2. (Continued)

36	<i>Narceus annularis</i>	0.21	0.20	0.20	0.21	0.21	0.21	0.21	0.22	0.23	0.20	0.21	0.22	0.21	0.20	0.20	0.21	0.21	0.20	0.24	0.22	0.23	0.21	0.23	0.22	0.22	0.23	0.22	0.22	0.21	0.21	0.20	0.20	0.21	0.20												
37	<i>Parabolus dimorphus</i> Pd34	0.21	0.21	0.22	0.19	0.19	0.19	0.20	0.21	0.18	0.20	0.19	0.22	0.18	0.20	0.21	0.19	0.21	0.19	0.22	0.18	0.22	0.19	0.18	0.20	0.20	0.20	0.17	0.19	0.18	0.25	0.21	0.19	0.18	0.20	0.17	0.20										
38	<i>Pelmatojulus tigrinus</i> Pt2	0.18	0.18	0.19	0.18	0.17	0.19	0.17	0.18	0.22	0.22	0.20	0.23	0.22	0.23	0.22	0.22	0.22	0.16	0.23	0.20	0.20	0.20	0.21	0.22	0.22	0.22	0.20	0.21	0.19	0.24	0.19	0.20	0.20	0.20	0.18	0.19	0.19									
39	<i>Pelmatojulus togoensis</i> Pto6	0.19	0.20	0.18	0.18	0.17	0.17	0.18	0.20	0.21	0.22	0.22	0.22	0.20	0.20	0.21	0.20	0.21	0.17	0.22	0.19	0.20	0.20	0.19	0.19	0.21	0.20	0.20	0.20	0.18	0.25	0.18	0.18	0.18	0.19	0.19	0.20	0.18	0.17								
40	<i>Pseudospirobolellus avernus</i> GPG	0.21	0.19	0.23	0.19	0.20	0.20	0.20	0.22	0.21	0.22	0.22	0.23	0.21	0.23	0.22	0.23	0.23	0.20	0.23	0.20	0.21	0.20	0.21	0.20	0.21	0.21	0.20	0.20	0.21	0.22	0.19	0.23	0.21	0.21	0.21	0.22	0.23	0.20	0.21							
41	<i>Pseudospirobolellus</i> KCS	0.22	0.22	0.22	0.22	0.22	0.21	0.23	0.23	0.23	0.23	0.21	0.23	0.23	0.22	0.22	0.23	0.23	0.22	0.23	0.22	0.22	0.21	0.21	0.22	0.22	0.23	0.22	0.22	0.22	0.21	0.23	0.22	0.22	0.24	0.22	0.21	0.22	0.22	0.14							
42	<i>Rhinocricus parvus</i> Rp49	0.24	0.23	0.23	0.23	0.23	0.22	0.23	0.24	0.24	0.21	0.22	0.22	0.24	0.21	0.23	0.22	0.23	0.22	0.25	0.25	0.25	0.25	0.25	0.25	0.25	0.25	0.24	0.25	0.24	0.22	0.22	0.22	0.23	0.23	0.22	0.20	0.23	0.21	0.22	0.22	0.21					
43	<i>Trachelomegalus</i> sp. Tr54	0.20	0.19	0.20	0.19	0.19	0.20	0.20	0.22	0.19	0.18	0.17	0.20	0.19	0.18	0.18	0.18	0.18	0.20	0.22	0.21	0.22	0.24	0.23	0.22	0.22	0.23	0.24	0.22	0.23	0.24	0.21	0.18	0.17	0.15	0.21	0.21	0.21	0.19	0.21	0.22	0.20	0.22				
44	<i>Trigoniulus corallinus</i> Tco15	0.15	0.14	0.13	0.13	0.13	0.14	0.12	0.12	0.18	0.19	0.20	0.23	0.19	0.20	0.20	0.21	0.21	0.17	0.20	0.18	0.18	0.17	0.18	0.19	0.17	0.18	0.17	0.17	0.16	0.23	0.14	0.18	0.16	0.17	0.18	0.20	0.19	0.18	0.17	0.23	0.22	0.23	0.20			
45	<i>Anurostreptus barthelemyae</i> Tib	0.21	0.21	0.22	0.20	0.20	0.19	0.21	0.22	0.22	0.22	0.23	0.24	0.23	0.22	0.24	0.23	0.24	0.20	0.25	0.19	0.21	0.19	0.19	0.20	0.19	0.20	0.19	0.19	0.18	0.23	0.22	0.21	0.20	0.22	0.22	0.21	0.21	0.21	0.20	0.22	0.21	0.23	0.23	0.19		
46	<i>Chonecambala crassicauda</i>	0.23	0.22	0.21	0.22	0.22	0.21	0.21	0.23	0.24	0.24	0.24	0.23	0.24	0.23	0.24	0.22	0.24	0.22	0.26	0.23	0.23	0.22	0.23	0.22	0.22	0.23	0.22	0.22	0.21	0.23	0.21	0.23	0.22	0.24	0.24	0.23	0.21	0.22	0.24	0.23	0.23	0.22	0.22	0.19		
47	<i>Thyropygus allevatus</i> Bb	0.21	0.21	0.21	0.20	0.21	0.20	0.21	0.22	0.21	0.21	0.22	0.23	0.23	0.23	0.22	0.21	0.24	0.20	0.23	0.20	0.19	0.20	0.20	0.19	0.19	0.20	0.19	0.20	0.19	0.22	0.20	0.21	0.20	0.22	0.21	0.20	0.21	0.23	0.21	0.22	0.22	0.21	0.24	0.20	0.15	0.20

Table 3. Estimates of 16S ribosomal RNA sequence divergences (uncorrected p-distances) within and among Trigoniulinae species and related taxa (rounded to two decimal places).

1	<i>Apeuthes pollex</i> , sp. nov. SML	1	2	3	4	5	6	7	8	9	10	11	12	13	14	15	16	17	18	19	20	21	22	23	24	25	26	27	28	29	30	31	32	33	34	35	36	37	38	39	40	41	42										
2	<i>Apeuthes pollex</i> , sp. nov. VTS	0.04																																																			
3	<i>Apeuthes longiligulatus</i> , sp. nov. TPP	0.11	0.09																																																		
4	<i>Apeuthes pollex</i> , sp. nov. SMR	0.05	0.02	0.09																																																	
5	<i>Apeuthes fimbriatus</i> , sp. nov. BMP	0.13	0.11	0.09	0.10																																																
6	? <i>Apeuthes spininavis</i> , sp. nov. ABB	0.15	0.13	0.12	0.13	0.13																																															
7	<i>Apeuthes maculatus</i> Amc	0.11	0.09	0.09	0.09	0.12	0.13																																														
8	<i>Apeuthes maculatus</i> Am26	0.08	0.06	0.07	0.06	0.10	0.11	0.03																																													
9	<i>Atopochetus dollfusii</i> DOL	0.19	0.17	0.19	0.19	0.22	0.21	0.19	0.18																																												
10	<i>Atopochetus helix</i> SPT	0.20	0.17	0.19	0.18	0.21	0.22	0.19	0.18	0.05																																											
11	<i>Atopochetus mouleimensis</i> TAK	0.21	0.19	0.20	0.20	0.23	0.22	0.20	0.19	0.07	0.06																																										

(Continued on next page)

Table 3. (Continued)

12	<i>Atopochetus setiferus</i> HPT	0.21	0.20	0.20	0.20	0.24	0.23	0.21	0.20	0.07	0.06	0.06																																														
13	<i>Atopochetus spinimargo</i> Ton27	0.19	0.17	0.18	0.17	0.21	0.21	0.19	0.18	0.07	0.06	0.06	0.07																																													
14	<i>Atopochetus truncatus</i> SML	0.19	0.17	0.18	0.17	0.22	0.22	0.19	0.18	0.05	0.05	0.07	0.07	0.05																																												
15	<i>Atopochetus uncinatus</i> KMR	0.19	0.18	0.19	0.18	0.21	0.21	0.18	0.17	0.04	0.04	0.06	0.07	0.06	0.05																																											
16	<i>Atopochetus weseneri</i> Tos29	0.20	0.18	0.19	0.19	0.22	0.22	0.20	0.19	0.06	0.05	0.07	0.05	0.06	0.03	0.05																																										
17	<i>Aulacobolus uncopygus</i> Auc	0.23	0.20	0.20	0.21	0.21	0.21	0.19	0.19	0.16	0.16	0.15	0.15	0.15	0.16	0.15	0.16																																									
18	<i>Coxobolellus albiceps</i> Stpw	0.26	0.26	0.27	0.26	0.28	0.28	0.28	0.26	0.22	0.23	0.23	0.24	0.22	0.22	0.23	0.23	0.26																																								
19	<i>Coxobolellus compactogonus</i> SKR	0.26	0.25	0.25	0.25	0.26	0.25	0.25	0.24	0.22	0.23	0.23	0.23	0.21	0.22	0.22	0.23	0.23	0.14																																							
20	<i>Coxobolellus fuscus</i> HKK	0.24	0.24	0.25	0.24	0.26	0.25	0.24	0.24	0.20	0.22	0.22	0.22	0.21	0.22	0.21	0.23	0.24	0.12	0.09																																						
21	<i>Coxobolellus nodosus</i> SPW	0.24	0.23	0.24	0.24	0.26	0.24	0.23	0.22	0.21	0.23	0.23	0.23	0.21	0.21	0.21	0.22	0.24	0.12	0.12	0.11																																					
22	<i>Coxobolellus serratus</i> KKL	0.26	0.24	0.25	0.24	0.27	0.25	0.25	0.24	0.21	0.22	0.23	0.22	0.21	0.21	0.22	0.22	0.23	0.13	0.10	0.09	0.13																																				
23	<i>Coxobolellus tenebris</i> TPL	0.26	0.24	0.24	0.25	0.25	0.25	0.24	0.23	0.22	0.23	0.23	0.23	0.22	0.23	0.22	0.23	0.23	0.15	0.07	0.09	0.12	0.10																																			
24	<i>Coxobolellus tigris</i> TYE	0.25	0.24	0.24	0.24	0.25	0.25	0.26	0.24	0.21	0.23	0.24	0.23	0.22	0.22	0.22	0.24	0.24	0.13	0.09	0.08	0.12	0.07	0.09																																		
25	<i>Coxobolellus transversalis</i> Stpg	0.24	0.23	0.24	0.23	0.26	0.25	0.24	0.24	0.20	0.21	0.21	0.21	0.21	0.21	0.21	0.22	0.23	0.10	0.11	0.09	0.09	0.11	0.11	0.12																																	
26	<i>Coxobolellus valvatus</i> BRC	0.23	0.22	0.24	0.23	0.25	0.24	0.23	0.22	0.20	0.21	0.22	0.22	0.20	0.20	0.21	0.21	0.23	0.10	0.11	0.09	0.05	0.11	0.11	0.11	0.07																																
27	<i>Leptogoniulus sorornus</i> BTN	0.16	0.13	0.15	0.13	0.15	0.15	0.10	0.12	0.22	0.21	0.23	0.23	0.22	0.22	0.22	0.22	0.21	0.29	0.27	0.25	0.26	0.25	0.27	0.26	0.26	0.25																															
28	<i>Litostrophus chamaeleon</i> PPT	0.23	0.21	0.22	0.21	0.24	0.24	0.21	0.20	0.10	0.11	0.12	0.10	0.11	0.11	0.11	0.10	0.14	0.23	0.22	0.21	0.22	0.21	0.21	0.22	0.22	0.22	0.22																														
29	<i>Litostrophus saraburensis</i> PKS	0.22	0.20	0.22	0.20	0.24	0.23	0.21	0.20	0.11	0.10	0.11	0.11	0.11	0.11	0.10	0.10	0.15	0.25	0.24	0.23	0.25	0.22	0.24	0.24	0.22	0.24	0.22	0.08																													
30	<i>Litostrophus scaber</i> Sca	0.22	0.19	0.22	0.20	0.22	0.21	0.21	0.20	0.10	0.11	0.11	0.11	0.10	0.10	0.10	0.10	0.14	0.25	0.22	0.22	0.22	0.21	0.22	0.22	0.22	0.22	0.23	0.09	0.06																												
31	<i>Litostrophus segregatus</i> Ls19	0.24	0.21	0.22	0.21	0.23	0.24	0.22	0.21	0.12	0.11	0.12	0.11	0.11	0.11	0.11	0.11	0.15	0.25	0.23	0.23	0.24	0.22	0.24	0.24	0.22	0.24	0.23	0.10	0.06	0.08																											
32	<i>Madabolus maximus</i> Mm4	0.22	0.21	0.21	0.21	0.22	0.24	0.21	0.21	0.19	0.18	0.19	0.19	0.17	0.19	0.17	0.20	0.19	0.24	0.23	0.24	0.23	0.25	0.24	0.26	0.22	0.22	0.22	0.19	0.21	0.22	0.20																										
33	<i>Parabolus dimorphus</i> Pd34	0.23	0.21	0.22	0.22	0.23	0.23	0.21	0.21	0.17	0.17	0.16	0.18	0.17	0.18	0.16	0.18	0.18	0.25	0.24	0.25	0.24	0.26	0.26	0.26	0.25	0.24	0.24	0.19	0.21	0.19	0.21	0.11																									
34	<i>Pelmatojulus tigrinus</i> Pt2	0.26	0.25	0.23	0.25	0.26	0.26	0.23	0.23	0.21	0.21	0.20	0.20	0.19	0.20	0.20	0.21	0.20	0.27	0.25	0.26	0.25	0.25	0.26	0.27	0.25	0.24	0.26	0.21	0.21	0.22	0.22	0.12	0.12																								
35	<i>Pelmatojulus togoensis</i> Pto6	0.24	0.22	0.22	0.23	0.22	0.24	0.21	0.21	0.19	0.19	0.19	0.18	0.17	0.19	0.17	0.19	0.18	0.27	0.25	0.26	0.25	0.25	0.27	0.27	0.26	0.25	0.24	0.21	0.22	0.20	0.20	0.11	0.09	0.12																							
36	<i>Pseudospirobolellus avernus</i> GPG	0.26	0.24	0.24	0.24	0.25	0.23	0.23	0.23	0.23	0.24	0.24	0.24	0.22	0.24	0.22	0.23	0.22	0.22	0.19	0.21	0.21	0.21	0.21	0.19	0.20	0.25	0.21	0.24	0.22	0.25	0.24	0.24	0.26	0.26																							
37	<i>Pseudospirobolellus</i> KCS	0.28	0.25	0.25	0.26	0.27	0.25	0.26	0.26	0.24	0.25	0.24	0.24	0.22	0.25	0.25	0.24	0.23	0.23	0.23	0.21	0.22	0.22	0.22	0.22	0.21	0.21	0.26	0.23	0.25	0.24	0.26	0.25	0.26	0.25	0.26	0.09																					
38	<i>Rhinocriscus parvus</i> Rp49	0.23	0.22	0.23	0.22	0.24	0.25	0.23	0.22	0.22	0.22	0.20	0.22	0.21	0.23	0.22	0.23	0.21	0.29	0.26	0.26	0.28	0.28	0.26	0.27	0.27	0.26	0.25	0.22	0.23	0.20	0.22	0.24	0.24	0.25	0.22	0.28	0.26																				
39	<i>Trachelomegalus cf. hoplurus</i> Th23	0.22	0.20	0.21	0.20	0.23	0.22	0.19	0.19	0.12	0.12	0.14	0.14	0.13	0.13	0.12	0.12	0.15	0.26	0.24	0.25	0.23	0.24	0.24	0.24	0.24	0.23	0.21	0.13	0.11	0.11	0.12	0.20	0.19	0.22	0.21	0.22	0.25	0.24																			
40	<i>Trigoniulus corallinus</i> Tco15	0.15	0.13	0.12	0.13	0.14	0.16	0.11	0.11	0.20	0.20	0.22	0.21	0.21	0.21	0.20	0.22	0.22	0.27	0.26	0.24	0.24	0.24	0.24	0.25	0.25	0.23	0.24	0.13	0.21	0.21	0.21	0.21	0.22	0.21	0.25	0.23	0.25	0.27	0.24	0.20																	
41	<i>Anurostreptus barthelemyae</i> Tlb	0.24	0.21	0.22	0.22	0.24	0.23	0.21	0.21	0.19	0.21	0.22	0.22	0.22	0.20	0.20	0.21	0.20	0.28	0.24	0.24	0.23	0.24	0.24	0.26	0.24	0.22	0.24	0.19	0.19	0.18	0.21	0.24	0.23	0.26	0.24	0.25	0.27	0.26	0.20	0.23																	
42	<i>Chonecambala crassicauda</i> Ttp	0.24	0.21	0.21	0.22	0.24	0.26	0.22	0.22	0.20	0.20	0.21	0.21	0.21	0.19	0.21	0.20	0.19	0.29	0.27	0.28	0.26	0.28	0.27	0.26	0.26	0.27	0.23	0.23	0.22	0.21	0.22	0.23	0.25	0.24	0.24	0.27	0.26	0.25	0.21	0.25	0.22																
43	<i>Thyropygus allevatus</i> Bb	0.23	0.20	0.21	0.21	0.23	0.23	0.21	0.20	0.23	0.23	0.24	0.23	0.22	0.23	0.22	0.23	0.20	0.27	0.25	0.24	0.26	0.26	0.25	0.26	0.25	0.26	0.23	0.23	0.24	0.22	0.24	0.25	0.23	0.25	0.24	0.26	0.28	0.28	0.23	0.20	0.14	0.23															

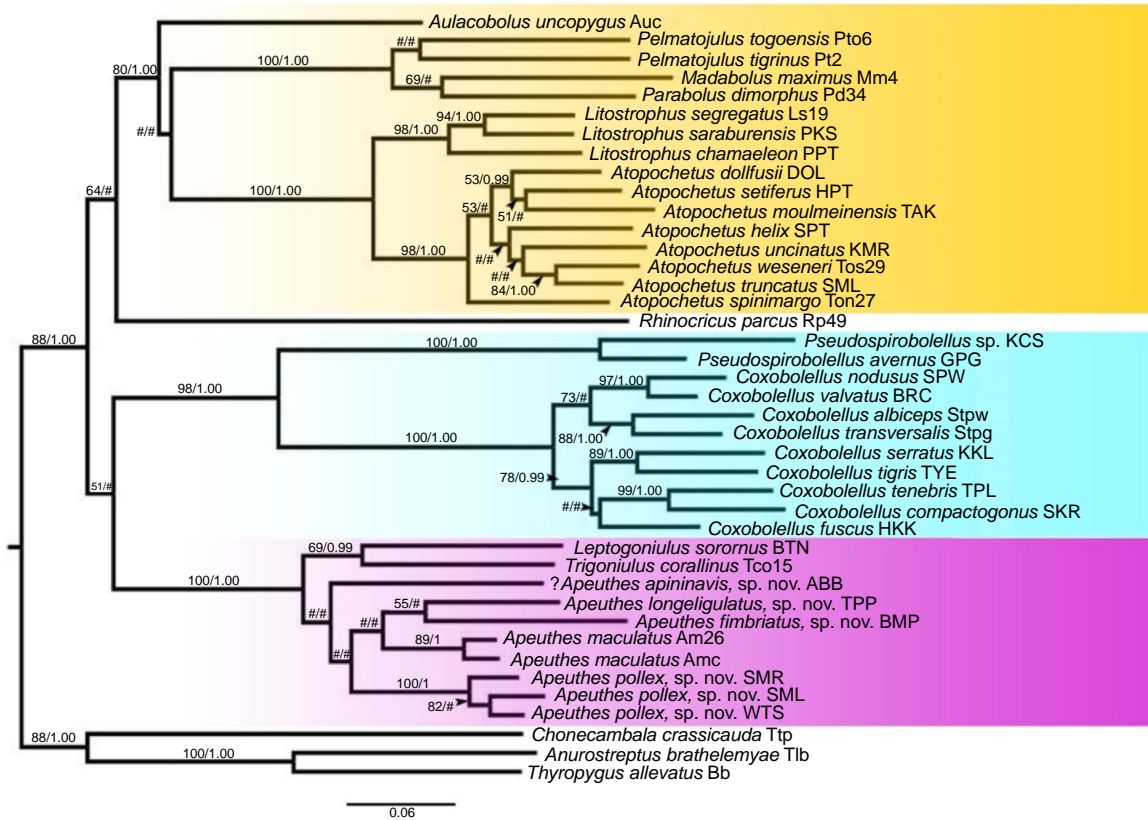


Fig. 1. Phylogenetic relationships of subfamily Trigoniulinae based on maximum likelihood analysis (ML) and Bayesian Inference (BI) of concatenated cytochrome c oxidase I (COI) + 16S ribosomal RNA alignment (1118 bp). Numbers at nodes indicate branch support based on bootstrapping (ML)/posterior probabilities (BI). Scale bar: 0.06 substitutions per site. The hash (#) indicates branches with <50% ML bootstrap support and <0.95 Bayesian posterior probability. The coloured area marks the Trigoniulinae species (purple), Pseudospirobolellidae species (light blue), and non-trigoniuline Pachybolidae species (yellow).

Table 4. Numbers of clusters and entities detected within the genus *Apeuthes* by the General Mixed Yule Coalescent (GMYC) method applied to the cytochrome c oxidase I (COI) dataset.

Analysis	Clusters (CI)	Entities (CI)	Likelihood null	Likelihood GMYC	Likelihood ratio	Threshold
Single	2 (1–3)	3 (1–7)	21.9968	23.1135	2.233348	–0.08547836
Multiple	2 (1–2)	4 (1–4)	21.9968	23.5326	3.071466	–0.08734653
						–0.02068326

species) were lower than the ML value of the GMYC model (Table 4). The single threshold yielded two clusters and three entities with confidence intervals (CI) ranging from 1 to 7. In this way, the following entities are recognised (1) *A. pollex*, sp. nov. SMR + *A. pollex*, sp. nov. WTS + *A. pollex*, sp. nov. SML, (2) ?*A. spininavis*, sp. nov., and (3) *A. maculatus* Amc + *A. maculatus* Am26 + *A. fimbriatus*, sp. nov. + *A. longeligulatus*, sp. nov. The multiple thresholds yielded two clusters and four entities with CI ranging from 1 to 4, so that the following species are recognised as entities (1) *A. pollex*, sp. nov. SMR + *A. pollex*, sp. nov. WTS + *A. pollex*, sp. nov. SML + ?*A. spininavis*, sp. nov.,

(2) *A. maculatus* Amc + *A. maculatus* Am26, (3) *A. fimbriatus*, sp. nov., and (4) *A. longeligulatus*, sp. nov. By combining these GMYC results with morphological data and considering the large interspecific sequence divergences of 11–16% (mean: 14%), we thus delimit five species, viz *A. maculatus*, *A. fimbriatus*, sp. nov., *A. longeligulatus*, sp. nov., *A. pollex*, sp. nov. and ?*A. spininavis*, sp. nov.

ASAP

Seven operational taxonomic units (OTUs) were found with a probability of 1.00 with recursive split *P*-value of 0.01 (Table 5). These seven OTUs are: (1) *A. longeligulatus*,

Table 5. Number of species delimited by the Poisson Tree Process (PTP) method and numbers of putative species delimited by the Assemble Species by Automatic Partitioning (ASAP) method applied to the cytochrome c oxidase I (COI) dataset of the genus *Apeuthes*.

Group	ASAP	PTP
1. <i>A. longeligulatus</i> , sp. nov. TPP	+	+
2. <i>A. spininavis</i> , sp. nov. ABB	+	+
3. <i>A. fimbriatus</i> , sp. nov. BMP	+	+
4. <i>A. pollex</i> , sp. nov. SML	+	–
5. <i>A. pollex</i> , sp. nov. WTS	+	–
6. <i>A. pollex</i> , sp. nov. SMR	+	–
7. <i>A. pollex</i> , sp. nov. SML + <i>A. pollex</i> , sp. nov. WTS + <i>A. pollex</i> , sp. nov. SMR	–	+
8. <i>Apeuthes maculatus</i> Amc, <i>Apeuthes maculatus</i> Am26	+	+

Note: abbreviations after species names refer to the isolate of each sequence as shown in Table 1. +, Molecular Operational Taxonomic Units supported as a putative species.

sp. nov., (2) ?*A. spininavis*, sp. nov. (3) *A. fimbriatus*, sp. nov., (4) *A. pollex*, sp. nov. SML, (5) *A. pollex*, sp. nov. WTS, (6) *A. pollex*, sp. nov. SMR, and (7) *A. maculatus* Amc + *A. maculatus* Am26. Yet, as the three *A. pollex*, sp. nov. OTUs have identical gonopods and show COI sequence divergences of 4–7% (mean: 5.7%), we regard them as a single OTU and thus retain five species in total.

PTP

Species delimitation results from PTP suggest five species (estimated number of species is between 1 and 8 species, mean: 5.34; Table 5) viz (1) *A. fimbriatus*, sp. nov. (2) ?*A. spininavis*, sp. nov., (3) *A. pollex*, sp. nov. SMR + *A. pollex*, sp. nov. SML + *A. pollex*, sp. nov. WTS, (4) *A. maculatus* Amc + *A. maculatus* Am26, and (5) *A. longeligulatus*, sp. nov.

Taxonomy

Class **DIPLOPODA** de Blainville in Gervais, 1844

Order **SPIROBOLIDA** Bollman, 1893

Suborder **TRIGONIULIDEA** Attems, 1909

Family **PACHYBOLIDAE** Cook, 1897

Subfamily **TRIGONIULINAE** Attems, 1909

Genus ***Apeuthes*** Hoffman & Keeton, 1960

Apeuthes Attems, 1938; invalidly proposed (as subgenus of *Eucarla* Brölemann, 1913)

Type species

Eucarla (*Apeuthes*) *maculata* Attems, 1938.

Included species

Apeuthes eydouxii (Gervais, 1847) (formerly *Iulus eydouxii* Gervais, 1847 and *Eucarla* (*Apeuthes*) *charactopyga* Attems, 1938), *Apeuthes exustus* (Attems, 1938) (formerly *Eucarla* (*Apeuthes*) *exusta* Attems, 1938), *Apeuthes maculatus* (Attems, 1938) (formerly *Eucarla* (*Apeuthes*) *maculata* Attems, 1938), *Apeuthes fimbriatus*, sp. nov., *Apeuthes longeligulatus*, sp. nov., *Apeuthes pollex*, sp. nov., ?*Apeuthes spininavis*, sp. nov.

Diagnosis

A genus of the pachybolid subfamily Trigoniulinae defined by having posterior gonopod telopodite with several dentate, serrate or tuberculate lamellae in a boat-like cavity (Attems 1938) or a boat-like cavity covered with spines (diagnostic extension provisionally added here to better accommodate ?*A. spininavis*, sp. nov., see Discussion).

General description (Fig. 2a–k)

Adult males with 50–62 podous rings, no apodous rings. Length ~5–7 cm, diameter ~3.5–4.9 mm. Adult females with 48–56 podous rings, no apodous rings. Length ~5–8 cm, diameter ~3.9–5.4 mm.

Head. Head capsule smooth. Occipital furrow extending down between, but not beyond eyes; clypeal furrow reaching level of antennal sockets. Area below antennal sockets and eyes impressed, forming part of antennal furrow. Incisura lateralis open. 2 + 2 labral teeth, a row of labral setae, 2 + 2 supralabral setae. Diameter of eyes approximately half of interocular space; 7–10 vertical rows of ommatidia, 7 horizontal rows, 40–46 ommatidia per eye. Antennae short, not reaching beyond collum when stretched back, accommodated in a shallow furrow composed of a horizontal segment in the head capsule and a vertical segment in the mandibular cardo and stipes. Antennomere lengths in *A. maculatus*, 2 > 6 > 3 > 4 = 5 > 1 > 7, in ?*A. spininavis*, sp. nov., 2 > 6 > 1 > 3 > 4 = 5 > 7, other species 2 > 6 > 1 > 5 > 3 = 4 > 7; antennomere 1 glabrous, 2 and 3 with some ventral setae, 4, 5 and 6 densely setose; 4 apical sensilla.

Mouthparts. Mandibles: stipes broad at base, apically gradually narrowed, with strong anterolateral marginal ridge. Gnathochilarium: each stipes with three apical setae; each lamella lingualis with two setae, one behind the other. Basal part of mentum transversely wrinkled; basal part of stipes longitudinally wrinkled.

Collum. Smooth, with a marginal furrow along lateral part of anterior margin; lateral lobes narrowly rounded, extending as far ventrad as the ventral margin of body ring 2 (slightly shorter than the ventral margin of body ring 2 in *A. pollex*, sp. nov.).

Body. Body rings 2–5 ventrally concave, hence with distinct ventrolateral ‘corners’. Body rings very smooth,

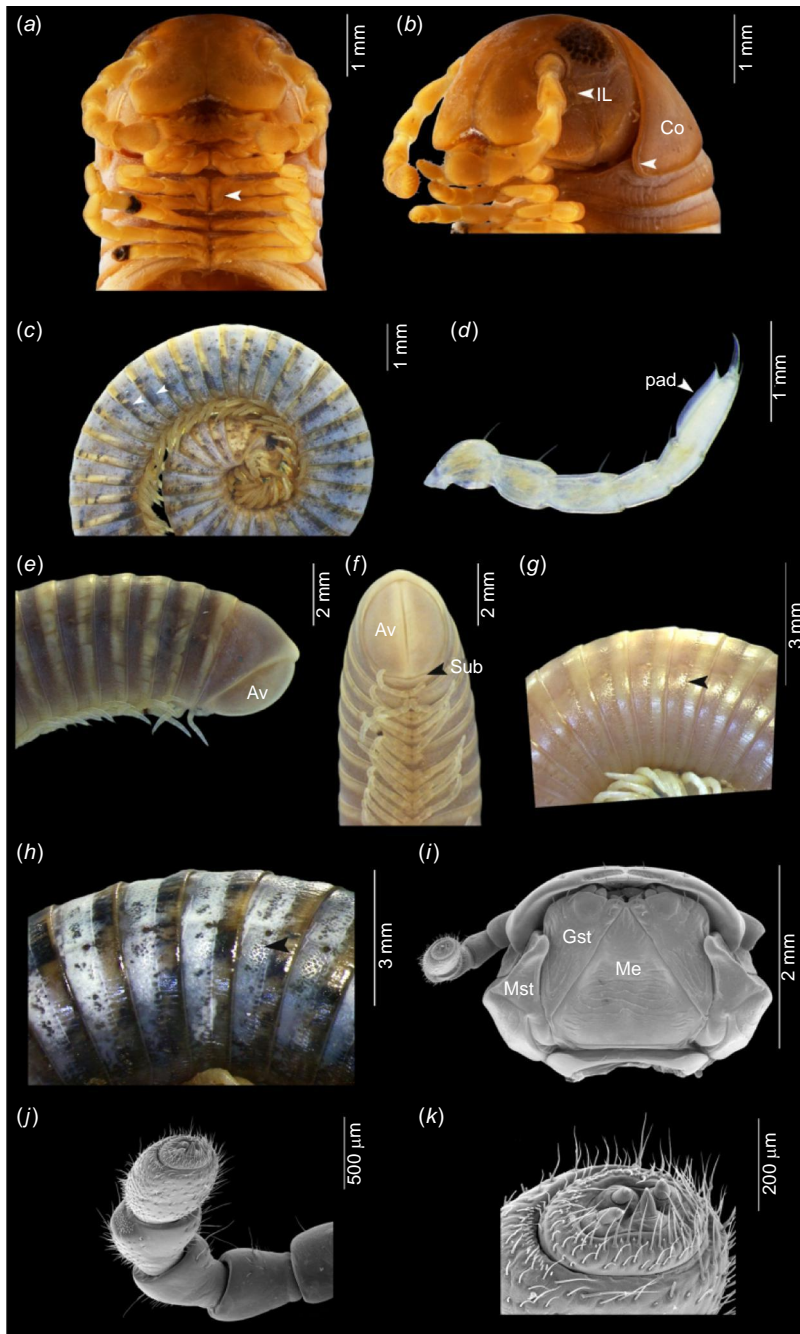


Fig. 2. External morphology of *Apeuthes* species. (a, b) *Apeuthes maculatus* (NHMW-Inv. No. 2395). (a) Anterior end, ventral view, arrow indicates the 3rd coxa process. (b) Anterior end, lateral view, arrow indicates incisura lateralis and collum. (c) *Apeuthes fimbriatus*, sp. nov. body rings, dorsal view. (d–g) *Apeuthes longeligulatus*, sp. nov. (d) Tarsal pad on male leg, lateral view. (e) Posterior end, lateral view. (f) Posterior end, ventral view. (g) Body rings, arrow indicates a row of punctate area between prozona and metazona, lateral view. (h) *Apeuthes fimbriatus*, sp. nov., body rings, arrow indicates punctate area on pro- and mesozona, lateral view. (i) *Apeuthes longeligulatus*, sp. nov. gnathochilarium, ventral view. (j, k) *Apeuthes pollex*, sp. nov. (j) Antenna, ventral view. (k) Tip of antenna, ventral view. Av, anal valves; Co, collum; Gst, gnathochilarium stipe; IL, incisura lateralis; Me, mentum; Mst, mandibles stipe; Pre, preanal ring; Sub, subanal scale.

parallel-sided in dorsal view. Prozona smooth in *A. maculatus*, *A. longeligulatus*, sp. nov. and *A. pollex*, sp. nov., whereas in *A. fimbriatus*, sp. nov. and ?*A. spininavis*, sp. nov. pro- and mesozona distinctly punctate. ‘Tergo-pleural’ suture visible on pro- and mesozona in *A. maculatus* and *A. pollex*, sp. nov.; mesozona ventrally with fine oblique striae (extending to dorsal parts and more distinct on ventral parts in *A. fimbriatus*, sp. nov.), dorsally punctate; metazona ventrally with fine longitudinal striae, otherwise smooth. ‘Pleural’ parts of rings with fine oblique striae. Sterna transversely striate. Ozopores from ring 6, situated in prozona,

~1 pore diameter in front of metazona. A punctate area around the rings between pro- and mesozona, forming a suture between pro- and metazona

Telson. Smooth; preanal ring with slightly concave dorsal profile, without process protruding beyond anal valves. Anal valves smooth, rounded (in *A. fimbriatus*, sp. nov., *A. pollex*, sp. nov. and ?*A. spininavis*, sp. nov. impressed submarginally; margins hence protruding, lip-like). Subanal scale broadly triangular.

Legs. Length of midbody legs 63–68% of body diameter in males, 47–52% of body diameter in females. Prefemur

basally constricted, tarsus longer than other podomeres. First and second legs with 1–2 prefemoral, 1–2 femoral, 1 postfemoral, and 2 tibial setae, and 4 ventral and 1 dorsal apical setae on tarsi, numbers of setae reaching constancy from pair 3: each leg podomere with 1 seta; tarsi in males with 1 ventral apical and 1 dorsal apical seta; females with 1 coxa, 1 prefemur, 1 femoral, 1 postfemoral, 1 tibial seta, tarsi with 1–3 ventral and 1 dorsal apical seta, the apical ventral seta larger than the more basal one.

Male sexual characters. Tarsus with large ventral soft pad occupying entire ventral surface from third to midbody legs in *A. longeligulatus*, sp. nov., to last legs in *A. fimbriatus*, sp. nov. and before the last 7–9 body rings in *A. pollex*, sp. nov. and ?*A. spininavis*, sp. nov. Body ring 7 entirely fused ventrally, no trace of a suture. Tip of anterior gonopods visible when the animal is stretched out (not when it is rolled up). With gonopod sternum. Posterior gonopods *in situ* completely hidden within anterior ones. Posterior gonopod telopodite apically concave forming a boat-like cavity.

Female vulvae. Large, *in situ* projecting beyond lateral extensions of coxosternum of 2nd legs. Operculum small, rounded triangular, situated at laterobasal end of vulva. Shape of valves variable.

Distribution

Malaysia, Thailand and Vietnam.

Species descriptions

Apeuthes fimbriatus, sp. nov.

(Fig. 3, 9)

<http://zoobank.org/urn:lsid:zoobank.org:act:D2C64473-D203-42A1-92BA-9402B9B5AD01>

<http://zoobank.org/urn:lsid:zoobank.org:pub:A897C3E7-9A6B-4037-B2FA-F85831635B30>

Material examined

Holotype: Male, VIETNAM, Da Nang Province, Bach Ma Peak, 16°07'49"N, 107°56'54"E. 29.iv.2007. S. Panha leg. (CUMZ-D00144-1).

Paratypes: 1 male (CUMZ-D00144), 2 females (CUMZ-D00144-2), same data as holotype.

Diagnosis

Differing from all other species in the genus by having a triangular mesal sternal process of anterior gonopod, not reaching so far as the tip of coxae (Fig. 3a, d). Anterior gonopod telopodite far overreaching coxa, distally bifid, forming a butterfly-like structure (Fig. 3b, e). Posterior gonopods apically with rounded and spiny lamellae, one above the other (Fig. 3f–h).

Description

Adult males with 53 podous rings. Length ~6–7 cm, diameter ~4.3–4.4 mm. Adult females with 53 podous rings. Length ~6 cm, diameter ~5.1–5.4 mm.

Colour in ethanol light brown, internal tissue dark brown and shining through the body (Fig. 2c, as indicated by arrows).

Anterior gonopods (Fig. 3a, b, d, e). Mesal sternal process triangular, not reaching so far as the tip of coxae, apical margin bilobed. Coxa oval, apically truncated, with obliquely higher margin mesally, projecting beyond sternal process. Telopodite far overreaching coxa, distally bifid, forming a butterfly-like structure; inner process slender, curving laterad, protruding higher than outer process; the outer process broadly rounded; basal part of telopodite with obliquely high ridge.

Posterior gonopods (Fig. 3c, f–i) curving mesad, with efferent canal (Enghoff 2011) running along mesal margin; apically with several flat lamellae in a boat-like cavity, with rounded and spiny lamellae mesally, one above the other; with a conical process covered with spinules, originating on mesal margin at telopodite midway; efferent canal terminating at base of this process.

Female vulvae (Fig. 3j). Valves simple, of equal size.

DNA barcode

The GenBank accession number of the *COI* barcode of the paratype is MZ567160 (voucher code CUMZ D00144).

Distribution

Da Nang Province, Vietnam (Fig. 9).

Etymology

The specific name is a Latin adjective, meaning ‘fringed’ and referring to the fringed lamella on the posterior gonopod.

Apeuthes longeligulatus, sp. nov.

(Fig. 4, 9)

<http://zoobank.org/urn:lsid:zoobank.org:act:7DD08734-05FB-4A8E-87C6-66F0BD5FEB48>

<http://zoobank.org/urn:lsid:zoobank.org:pub:A897C3E7-9A6B-4037-B2FA-F85831635B30>

Material examined

Holotype: Male, THAILAND, Sa Kao Province, Klong Hard District, Tham Phet Po Thong, 13°24'49"N, 102°19'31"E. 24.x.2010. P. Pimvichai leg. (CUMZ-D00140-1).

Paratypes: 1 male CUMZ-D00140, same data as holotype. 1 male, 1 female, THAILAND, Trad Province, Koh Chang District, Koh Chang, Khlong Phraa (should be Khlong Phraw beach), 12°03'49"N,

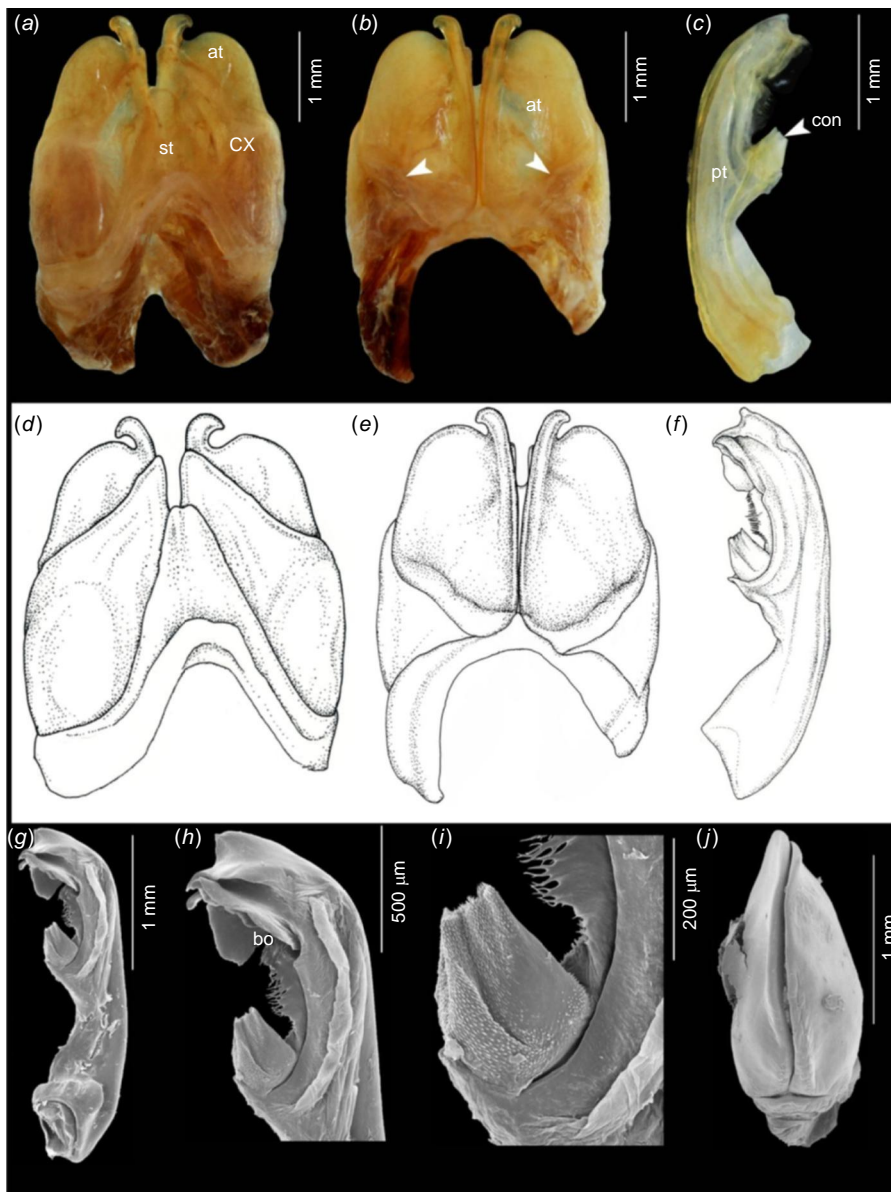


Fig. 3. *Apeuthes fimbriatus*, sp. nov., holotype, gonopods (specimen from Bach Ma Peak, CUMZ D00144-I). (a, d) Anterior gonopod, anterior view. (b, e) Anterior gonopod, posterior view. (c, f) Right, left posterior gonopod, respectively. (g) Scanning electron micrograph (SEM), left posterior gonopod, posterior–mesal view. (h) SEM, tip of posterior gonopod, mesal view. (i) SEM, conical process of posterior gonopod, dorsal view. (j) SEM, left female vulva, posterior mesal view. at, anterior gonopod telopodite; bo, boat-like cavity; con, conical process; cx, coxa; pt, posterior gonopod telopodite; st, sternum.

102°17'19"E. 31.viii.1990. Arne Redsted Rasmussen leg. (NHMD-621698).

Diagnosis

Differing from all other species in the genus by having a narrow mesal sternal process of anterior gonopod, protruding slightly higher than coxae (Fig. 4a, d). Anterior gonopod telopodite distally bifid (Fig. 4b, e). Posterior gonopods apically with several flattened lamellae in a boat-like cavity (Fig. 4c, f–i).

Description

Adult males with 56–62 podous rings. Length ~6–7 cm, diameter ~4.3–4.4 mm. Adult female with 56 podous rings. Length ~6 cm, diameter ~4.7 mm.

Colour in ethanol uniform brown; colour of living animal uniform reddish brown.

Anterior gonopods (Fig. 4a, b, d, e) with high, narrow mesal sternal process, protruding slightly higher than coxae; sternal process ending in a rounded lobe, with basal longitudinal triangular ridge on posterior side. Coxa oval, apically concave with two rounded lobes, the mesal one higher than the lateral one. Telopodite overreaching coxa, distally bifid, inner process slender, curving laterad; outer process broadly triangular; basal part of telopodite with a prominent transverse ridge.

Posterior gonopods (Fig. 4c, f–i) curving mesad, with efferent canal (Engghoff 2011) running along mesal margin; apically with several flattened lamellae in a boat-like cavity; with a conical process covered with spinules,

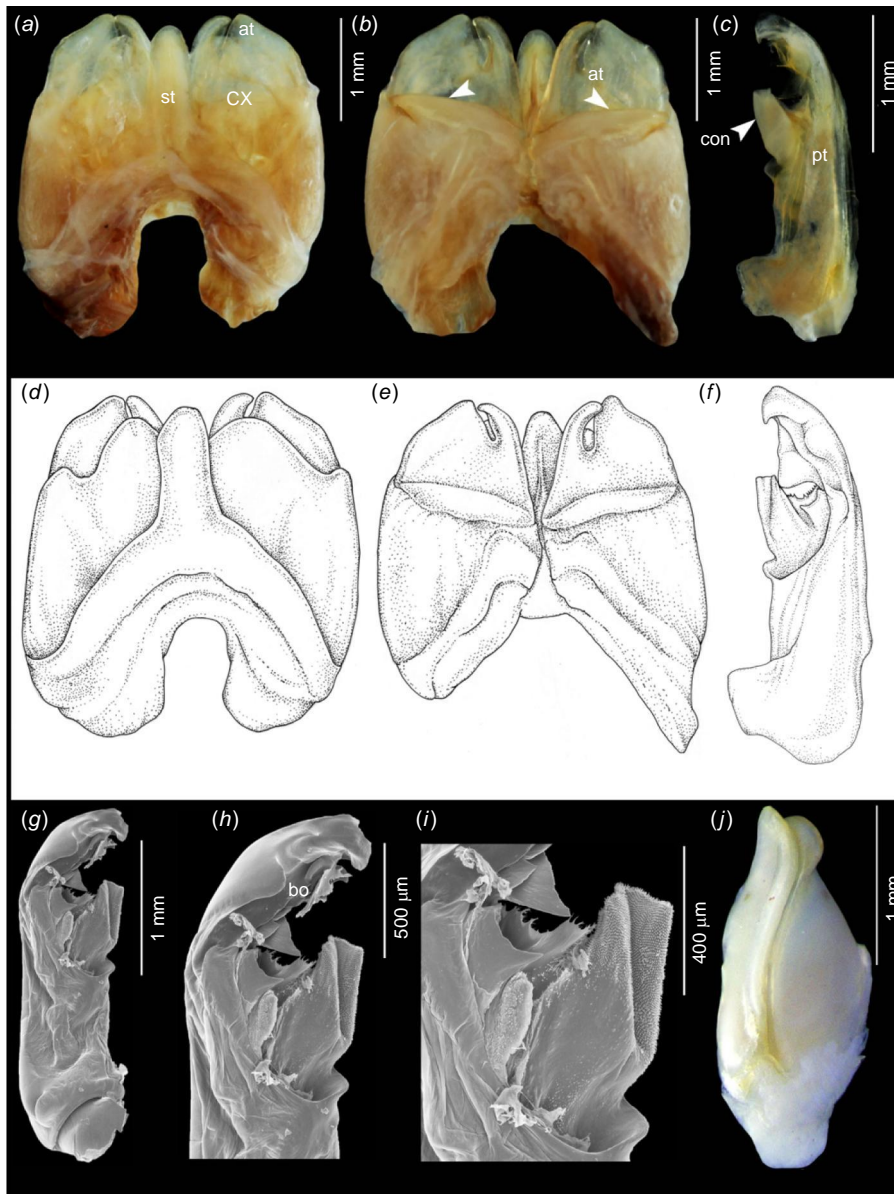


Fig. 4. *Apeuthes longeligulatus*, sp. nov., holotype, gonopods (specimen from Tham Phet Po Thong, CUMZ D00140-1). (a, d) Anterior gonopod, anterior view. (b, e) Anterior gonopod, posterior view. (c, f) Left posterior gonopod. (g) Scanning electron micrograph (SEM), right posterior gonopod, posterior–mesal view. (h) SEM, tip of posterior gonopod, mesal view. (i) SEM, conical process of posterior gonopod, dorsal view. (j) SEM, left female vulva, posterior mesal view. at, anterior gonopod telopodite; bo, boat-like cavity; con, conical process; cx, coxa; pt, posterior gonopod telopodite; st, sternum.

originating on mesal margin at telopodite midway; efferent canal terminating at base of this process.

Female vulvae (Fig. 4j). Valves simple, of equal size.

DNA barcode

The GenBank accession number of the *COI* barcode of the paratype is MZ567161 (voucher code CUMZ D00140).

Distribution

Sa Kaeo and Trad provinces, Thailand (Fig. 9).

Etymology

The specific name is a Latin adjective, meaning ‘with a long tongue’ and referring to the sternal process of the anterior gonopod.

Apeuthes pollex, sp. nov.

(Fig. 5, 8, 9)

<http://zoobank.org/urn:lsid:zoobank.org:act:AF851067-AEA7-4B6F-A65A-A573849A70F9>

<http://zoobank.org/urn:lsid:zoobank.org:pub:A897C3E7-9A6B-4037-B2FA-F85831635B30>

Material examined

Holotype: Male, THAILAND, Krabi Province, Muang District, Tham Sue Temple, 08°07'36"N, 98°55'27"E. 24.viii.2014. P. Pimvichai and T. Backeljau leg. (CUMZ-D00143-1).

Paratypes: 3 males (CUMZ-D00143), 2 females (CUMZ-D00143-3), same data as holotype. 1 male (CUMZ-D00141), THAILAND, Krabi,

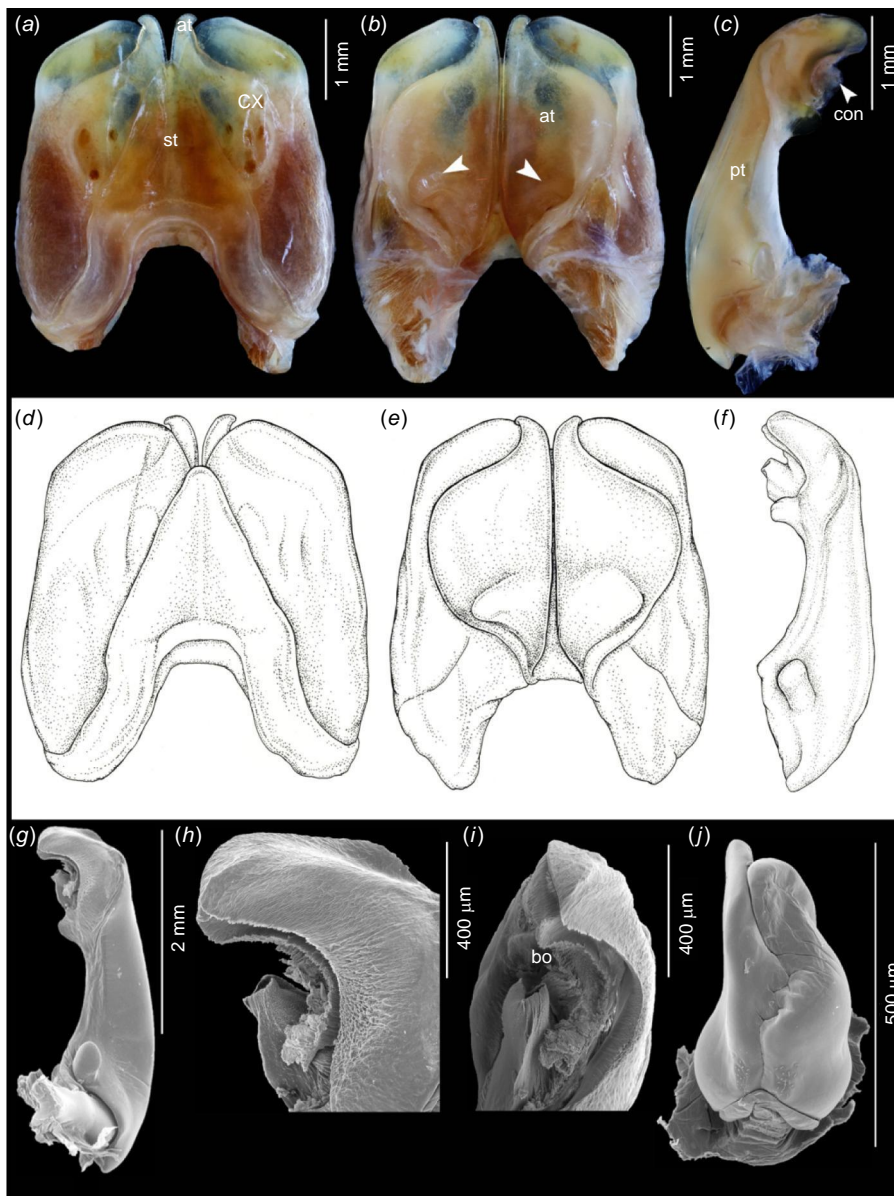


Fig. 5. *Apeuthes pollex*, sp. nov., holotype, gonopods (specimen from Tham Sue Temple, CUMZ D00143-I). (a, d) Anterior gonopod, anterior view. (b, e) Anterior gonopod, posterior view. (c, f) Right, left posterior gonopod, respectively. (g) Scanning electron micrograph (SEM), left posterior gonopod, posterior–mesal view. (h) SEM, conical process of posterior gonopod, mesal view. (i) SEM, tip of posterior gonopod, dorsal view. (j) SEM, left female vulva, posterior mesal view. at, anterior gonopod telopodite; bo, boat-like cavity; con, conical process; cx, coxa; pt, posterior gonopod telopodite; st, sternum.

Khlong Thom District, Sra Morakot, 07°55'31"N, 99°16'05"E. 24.viii.2014. P. Pimvichai and T. Backeljau leg. 2 males CUMZ-D00142), 1 female (CUMZ-D00142-2), THAILAND, Phang-Nga Province, Khuraburi District, Koh 8, Similan islands, 08°39'09"N, 97°38'27"E. 7.iv.2010. P. Pimvichai leg.

Diagnosis

Differing from all other species in the genus by having coxa of anterior gonopod distinctly concave for accommodation of telopodite (Fig. 5b, e). Anterior gonopod telopodite protruding slightly over coxa, apically abruptly narrowed, ending in one slender process (Fig. 5b, e). Posterior gonopods apically with a rounded lobe, with serrated lamellae mesally and with a thumb-like process basally (Fig. 5c, f, g).

Description

Adult males with 56–58 podous rings. Length ~6–7 cm, diameter ~4.8–4.9 mm. Adult females with 54–55 podous rings. Length ~8 cm, diameter ~5.4 mm.

Colour of living animal uniform reddish brown (Fig. 8).

Anterior gonopods (Fig. 5a, b, d, e) with broad, triangular mesal sternal process, not reaching so far as the tip of coxae. Coxa oval, projecting beyond sternal process, in posterior view concave for accommodation of telopodite. Telopodite protruding slightly over coxa, apically abruptly narrowed, forming a slender process, curving laterad, lateral margin thick and higher than mesal part and tip, basal part with a prominent ridge in the middle.

Posterior gonopods (Fig. 5c, f–i) curving mesad, apically with serrate lamellae in a boat-like cavity; with a conical process covered with setae near tip, originating from mesal margin, basally with a thumb-like process.

Female vulvae (Fig. 5j). Valves prominent, of equal size; free margins meeting in coarsely serrate suture; two valves fitting tightly together.

DNA barcode

The GenBank accession number of the COI barcode of the paratype is MZ567163 (voucher code CUMZ D00142).

Distribution

Krabi and Phang-Nga provinces, Thailand (Fig. 9).

Etymology

The specific epithet is a noun in apposition, meaning ‘thumb’ and referring to the thumb-like basal process on the posterior gonopod.

?Apeuthes spininavis, sp. nov.

(Fig. 6, 9)

<http://zoobank.org/urn:lsid:zoobank.org:act:FC08A14B-F4CB-4865-8847-2D6EEC48660B>

<http://zoobank.org/urn:lsid:zoobank.org:pub:A897C3E7-9A6B-4037-B2FA-F85831635B30>

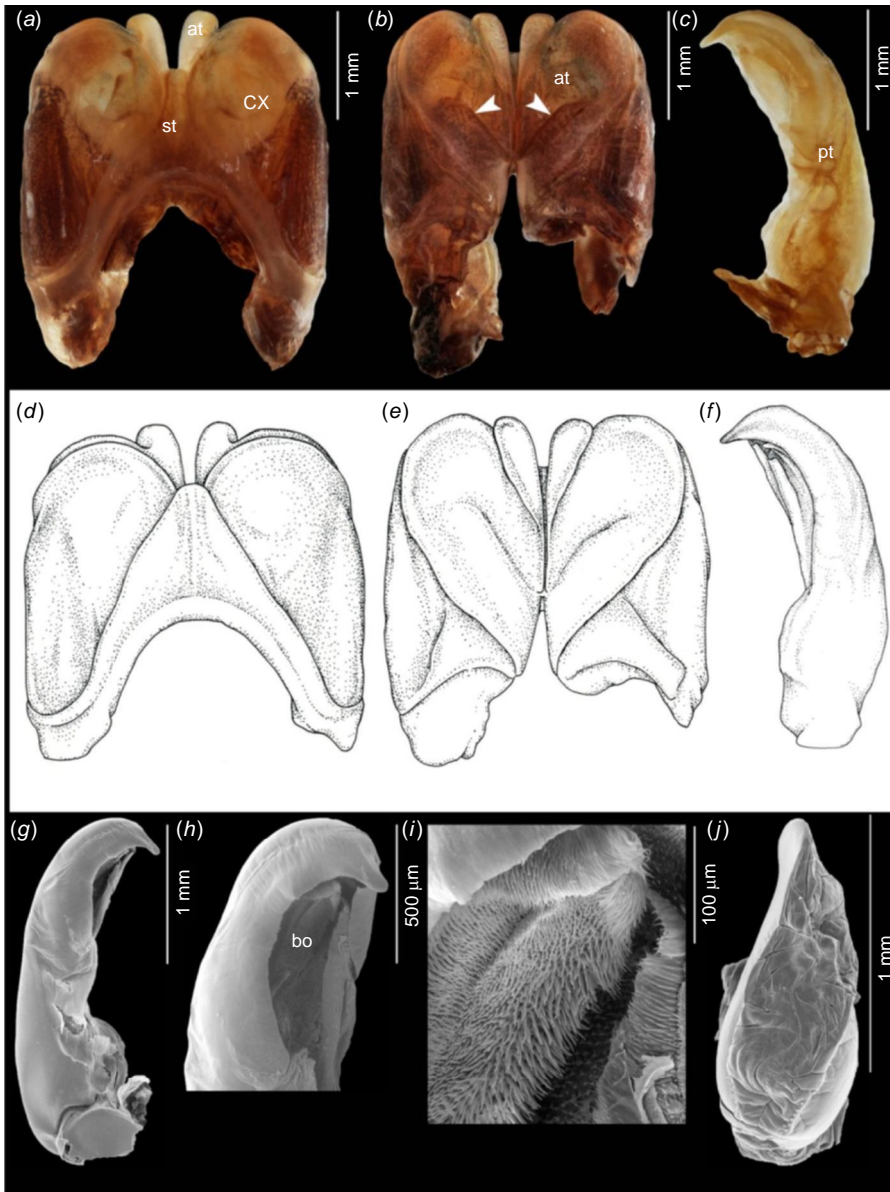


Fig. 6. *Apeuthes spininavis*, sp. nov., holotype, gonopods (specimen from Pulau Besar island, CUMZ D00146). (a, d) Anterior gonopod, anterior view. (b, e) Anterior gonopod, posterior view. (c, f) Left posterior gonopod. (g) Scanning electron micrograph (SEM), right posterior gonopod, posterior–mesal view. (h) SEM, tip of posterior gonopod, mesal view. (i) SEM, spine in boat-like cavity of posterior gonopod, dorsal view. (j) SEM, left female vulva, posterior mesal view. at, anterior gonopod telopodite; bo, boat-like cavity; cx, coxa; pt, posterior gonopod telopodite; st, sternum.

Material examined

Holotype: Male, MALAYSIA, Johor Province, Pulau Besar island, 02°26'3"N, 103°58'45"E. 2.iii.2008. P. Pimvichai, P. Prasankok and Ng Beewah leg. (CUMZ-D00146).

Paratypes: 1 male (CUMZ-D00146-1), 4 females (CUMZ-D00146-2), same data as holotype. 1 male (CUMZ-D00145), 1 female (CUMZ-D00145-1), MALAYSIA, Perak Province, Air Banun, 05°34'42"N, 101°25'58"E. 27.v.2011. P. Pimvichai, P. Prasankok and Ng Beewah leg.

Diagnosis

Anterior gonopods with broad, triangular mesal sternal process (Fig. 6a, d). Similar in this respect to *A. pollex*, sp. nov. Differing from all other *Apeuthes* species by having posterior gonopods that are apically abruptly narrowed, forming a pointed lobe (Fig. 6c, f–h), and with a mesal margin forming a deep boat-like cavity covered with spines (Fig. 6h, i) and without a conical process at mesal margin of posterior gonopod telopodite.

Description

Adult males with 50–56 podous rings. Length ~5–6 cm, diameter ~3.5–3.9 mm. Adult female with 48–55 podous rings. Length ~5–6 cm, diameter ~3.9–4.5 mm.

Colour in ethanol uniform brown, colour of living animal uniform reddish brown.

Anterior gonopods (Fig. 6a, b, d, e) with broad, triangular mesal sternal process, not reaching so far as the tip of coxae, with basal longitudinal triangular ridge. Coxa oval, projecting beyond sternal process, in posterior view concave for accommodation of telopodite. Telopodite protruding slightly over coxa, apically ending in two processes; inner process slender, curving obliquely laterad; outer process broadly rounded; basal part of telopodite with oblique high ridge in the middle.

Posterior gonopods (Fig. 6c, f–i) curving mesad, apically forming a deep boat-like cavity covered with spines, and distally abruptly narrowed, forming a pointed lobe.

Female vulvae (Fig. 6j). Valves prominent, of equal size; free margins meeting in coarsely serrate suture, soft area in the middle; two valves fitting tightly together.

DNA barcode

The GenBank accession number of the COI barcode of the paratype is MZ567165 (voucher code CUMZ D00145).

Distribution

Johor and Perak provinces, Malaysia (Fig. 9).

Etymology

The specific epithet is a noun in apposition, 'spiny boat', referring to the shape and texture of the posterior gonopod telopodite.

Note

?*Apeuthes spininavis*, sp. nov. shares several characters with other species in the genus *Apeuthes*. However, it differs from all of other species of *Apeuthes* by the absence of a conical process covered with spinules midway on the mesal margin of the posterior gonopod telopodite. Hence, for the time being, we only tentatively assign this species to *Apeuthes* and refer it to as ?*Apeuthes spininavis*, sp. nov.

Key to the species of *Apeuthes* (based on adult males)

- Posterior gonopods without a conical process at telopodite midway; tip of telopodite apically abruptly narrowed forming a pointed lobe (Fig. 6c, f, g), mesal margin forming a deep boat-like cavity covered with spines (Fig. 6i).....?*Apeuthes spininavis*, sp. nov.
Posterior gonopods with a conical process.....2
- Posterior gonopods without flagelloid solenomere.....3
Posterior gonopods with flagelloid solenomere (Fig. 7c, f).....5
- A conical process located near telopodite tip (Fig. 5c, f–i); the conical process covered with spinules; telopodite of anterior gonopod ending in one process, apically abruptly narrowed, forming a slender process (Fig. 5b, e).....*Apeuthes pollex*, sp. nov.
A conical process located at telopodite midway; telopodite of anterior gonopod ending in two processes.....4
- Anterior gonopod with narrow mesal sternal process (Fig. 4a, d), apical margin rounded; telopodite of anterior gonopod distally bifid (Fig. 4b, e), the inner process slender, protruding as high as the outer one; the outer process broadly triangular; mesal part of telopodite with a prominent transverse ridge (Fig. 4b, e).....*Apeuthes longiligulatus*, sp. nov.
Anterior gonopod with triangular mesal sternal process, apical margin bilobed (Fig. 3d); telopodite of anterior gonopod distally bifid, forming a butterfly-like structure (Fig. 3b, e); the inner process slender, protruding higher than the outer process; the outer process broadly rounded; basal part of telopodite with obliquely high ridge (Fig. 3b, e).....*Apeuthes fimbriatus*, sp. nov.
- Anterior gonopod coxa apically abruptly truncated; telopodite of posterior gonopod with relatively long bifid flagelloid solenomere, forming two sharp spines (fig. 123, 125, 126 of Attems 1938, p. 258).....*Apeuthes eydouxii* (Gervais, 1847)
Anterior gonopod coxa apically rounded or triangular; posterior gonopod telopodite with long, slender flagelloid solenomere.....6
- Telopodite of anterior gonopod protruding as high as coxa, apically ending in two processes (Fig. 7b); the inner process slender, triangular, directed laterad, protruding as high as the outer one; the outer process broadly rounded lobe; basal part of telopodite with a massive transverse ridge (Fig. 7b; fig. 127 of Attems 1938, p. 260).....*Apeuthes exustus* (Attems, 1938)
Telopodite of anterior gonopod protruding beyond coxa, apically ending in two well-separated processes (Fig. 7e); the inner process slender, triangular, directed laterad, protruding higher than the outer one; the outer process broadly rounded lobe; basal part of telopodite with a pointed, triangular ridge in the middle (Fig. 7e).....*Apeuthes maculatus* (Attems, 1938)

Discussion

The genus *Apeuthes* was first proposed as a subgenus of *Eucarlia* Brölemann, 1913 by Attems (1938), who,

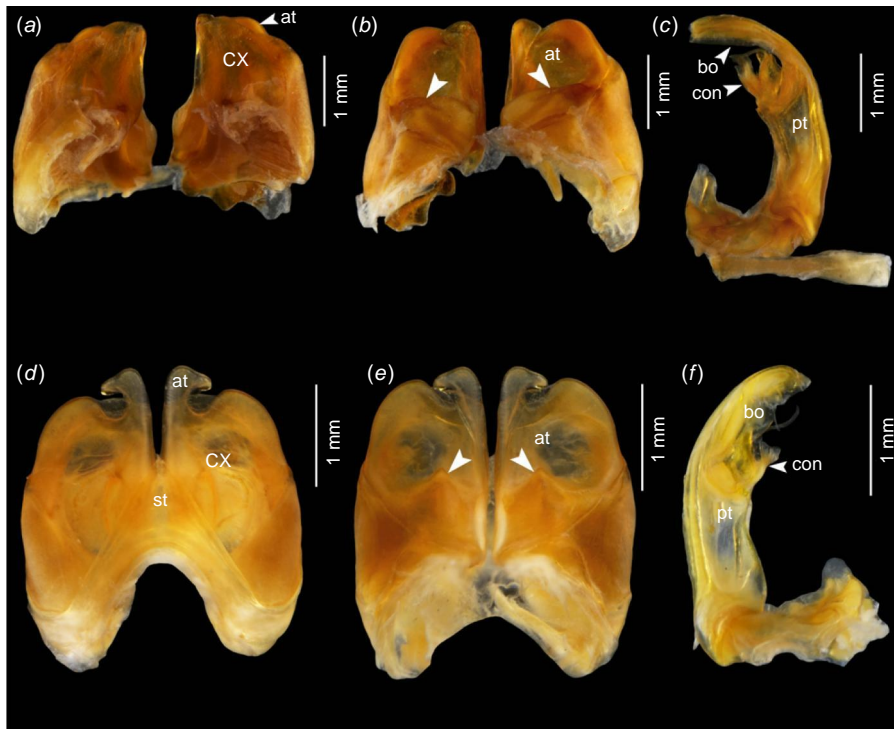


Fig. 7. *Apeuthes exustus* and *Apeuthes maculatus*, holotype, gonopods. (a–c) *Apeuthes exustus*, NHMW-Inv. No. 2394. (a) Anterior gonopod, anterior view. (b) Anterior gonopod, posterior view. (c) Right posterior gonopod. (d–f) *Apeuthes maculatus*, NHMW-Inv. No. 8440. (d) Anterior gonopod, anterior view. (e) Anterior gonopod, posterior view. (f) Left posterior gonopod. at, anterior gonopod telopodite; bo, boat-like cavity; con, conical process; cx, coxa; pt, posterior gonopod telopodite; st, sternum.



Fig. 8. Live *Apeuthes pollex*, sp. nov. from Tham Sue Temple (WTS), male (paratype, CUMZ D00143-2).

unfortunately, did not designate a type species for it. Hence the (sub)genus was invalid until Hoffman and Keeton (1960) designated *Eucarlia* (*Apeuthes*) *maculata* Attems, 1938, as its type species. Subsequently, Hoffman (1980) raised *Apeuthes* to full genus status without any rationale or explanation.

Attems (1938, pp. 259–260) characterised *Apeuthes* as follows (translated from German): the three just described species (our addition: (*Eucarlia* (*Apeuthes*) *charactopyga* Attems, 1938, *Eucarlia* (*Apeuthes*) *exusta* Attems, 1938 and *Eucarlia* (*Apeuthes*) *maculata* Attems, 1938)) have a peculiarity on the posterior gonopods that is missing in the other species of *Eucarlia*: the part of the gonopod distal

of the internal branch is longer than in the other species and has several dentate, serrate or tuberculate lamellae in the boat-like cavity.

Three new species described in the present study share the characters that Attems (1938) used to separate the subgenus *Apeuthes* from *Eucarlia*, viz the part of the posterior gonopod telopodite distal of the internal branch is long and has several dentate, serrate or tuberculate lamellae in the boat-like cavity. Therefore, we assign *A. fimbriatus*, sp. nov., *A. longeligulatus*, sp. nov. and *A. pollex*, sp. nov. without much hesitation to *Apeuthes*. Yet, while ?*A. spininavis*, sp. nov. shares the anterior gonopod telopodite with a distinct transverse ridge at its base, it lacks the long internal branch of the posterior gonopod telopodite and it has no dentate, serrate or tuberculate lamellae in the boat-like cavity on the posterior gonopod. Instead, it has a boat-like cavity that is covered with spines on the posterior gonopod. Therefore its assignment to *Apeuthes* is less obvious and is only provisionally proposed, in await of a more comprehensive revision of the genera *Apeuthes* and *Eucarlia*, and other related genera. In line with Art 11.9.3.4 of the International Commission on Zoological Nomenclature (<https://www.iczn.org/the-code/the-code-online/>), we thus cite this species as ?*Apeuthes spininavis*, sp. nov. and use a '?' to indicate the tentative nature of the generic assignment, as has been done before us for other tentative generic assignments (e.g. Golovatch and Korsós 1992). We prefer this conservative nomenclatural approach over creating a new monotypic genus for ?*A. spininavis* because the classification of the Pachybolidae 'is a real mess' (Golovatch and Korsós 1992,



Fig. 9. Distribution of the species of *Apeuthes*. The three described species' localities obtained from the original description. Droplets vary in size only to improve readability.

p. 12) and the family is still in need of revision (Enghoff *et al.* 2015), so that 'Prior to a thorough revision of this family, almost any generic allocation ought to be understood as temporary' (Golovatch and Korsós 1992, p. 12). Although this latter statement may be a bit exaggerated, it does imply that creating new pachybolid genera is likely to further complicate current nomenclature and future revisions. This may also apply to a new (monotypic) genus for ?*A. spininavis*, because it would be introduced only to express the relative phenotypic distinctiveness of this species, rather than to reflect the result of a sound phylogenetic framework, involving well founded phenotypic synapomorphies and DNA sequence analyses. Indeed, given the limited taxon and DNA marker sampling in our study, and considering the poor support of the *Apeuthes* relationships in our phylogenetic trees (Fig. 1 and Supplementary Fig. S1, S2), we do not see how pachybolid taxonomy and its users would be well served by the premature introduction of a new monotypic genus built on such ambiguous grounds. Conversely, if we extend Attems' (1938) diagnosis of *Apeuthes* by suggesting the 'boat-like cavity that is covered with spines on the posterior gonopod' of ?*A. spininavis* as a fourth defining character state of *Apeuthes*, next to 'the dentate, serrate or tuberculate lamellae

in the boat-like cavity', then the phenotypic distinctiveness of ?*A. spininavis* can, at least provisionally, be accommodated by the current concept of *Apeuthes* (but see further below). This idea is illustrated by Table 6 in which the morphological differences among *Apeuthes*, *Eucarlia* and the four new species are summarised. Thus, with our approach, we aim at complying with 'Taxon Naming Criterion 8' of Vences *et al.* (2013, p. 228): 'avoid oversplitting and deliberately creating monotypic taxa', a recommendation that is also made by other authors (e.g. Bickham *et al.* 2007; Kaiser *et al.* 2013) and instances (e.g. Australian Society of Herpetologists 2016).

The seven species here assigned to the genus *Apeuthes* show a considerable amount of interspecific morphological variation and differentiation. This is the case for: (1) the male 3rd leg pairs with a conical process projecting backwards, a condition that is only present in *A. maculatus* and *A. pollex*, sp. nov.; (2) the tarsal pads from the 3rd to the last legs, which are present only in males of *A. maculatus*, whereas there are no pads on the legs of the posterior rings in other species; (3) the lips of the anal valves being separated from the margin by a furrow in *A. exustus*, *A. fimbriatus*, sp. nov., *A. pollex*, sp. nov. and ?*A. spininavis*, sp. nov., whereas the lips of the anal valves connect directly to

each other (no furrow between the lips and the margin) in the other *Apeuthes* species; (4) the distinctly punctate prozona, which is present in *A. fimbriatus*, *A. longeligulatus*, sp. nov. and ?*A. spininavis*, sp. nov., but not in *A. maculatus* and *A. pollex*, sp. nov. (and not examined in *A. exustus* and *A. eydouxii*); and (5) the conical process on the posterior gonopod telopodite, which is present in all species except ?*A. spininavis*, sp. nov. It is unclear to what extent these patterns of morphological variation reflect phylogenetic relationships.

Next to the morphological heterogeneity in *Apeuthes*, there is also a substantial amount of *COI* sequence variation and differentiation, with intraspecific *COI* divergences of 3–7% (mean: 5%), and interspecific *COI* divergences of 11–16% (mean: 13.7%). These figures are in line with those for the genus *Coxobolellus* (Pimvichai, Enghoff, Panha & Backeljau, 2020) of the related family Pseudospirobolellidae, which has intraspecific *COI* divergences of 0–5% (mean: 2%) and interspecific *COI* divergences of 6–15% (mean: 11%) (Pimvichai et al. 2020). The corresponding values for the genera *Atopochetus* Attems, 1953 and *Litostrophus* Chamberlin, 1921 (family Pachybolidae) are also comparable, with intraspecific *COI* divergences of 0–8 and 0–1% (mean: 3 and 0%) respectively, and interspecific *COI* divergences of 9–17 and 9–11% (mean: 14 and 11%) respectively. Large *COI* sequence divergences are further observed in the genera *Thyropygus* Pocock, 1894 and *Anurostreptus* Attems, 1914 (Spirostreptida, Harpagophoridae) with intraspecific values of 0–12 and 0–6% (mean: 6 and 3%) respectively, and interspecific divergences of 5–18 and 9–11% (mean: 14 and 11%) respectively (Pimvichai et al. 2014). In the family Spirostreptidae Brandt, 1833, the intergeneric *COI* sequence divergences are 6.83–26.81% (mean: 18.43%) (Mwabvu et al. 2015). As such, the amounts of sequence differentiation among the four new *Apeuthes* species are approximately in line with species-level divergences in other spirostreptid and spirobolid genera.

The number of species delimited by ASAP exceeds the total number of morphospecies (seven ASAP species v. five morphospecies). However, five species were retained

because ASAP suggests *A. pollex*, sp. nov. from three different localities as three putative species. Yet, because they have identical gonopods and show sequence divergences of 4–7% (mean: 5.7%), we see no reason to recognise them as different species. This is in line with the PTP method, which also suggests five species, coinciding with the morphospecies. The single threshold GMYC method provides three entities (CI = 1–7), whereas the multiple threshold GMYC method provides four entities (CI = 1–4). GMYC thus suggests fewer species than we have distinguished, but the number of species that we separated is still well within the CI range of the single threshold GMYC method and close to the values provided by the multiple threshold GMYC method. By combining the GMYC results with the gonopodal characters, and in view of the large interspecific sequence divergences of 11–16% (mean: 14%), we thus delimit five species, so that in this group it appears that *COI* sequence divergences of >7%, accompanied by distinct gonopodal characters, seem to mark the transition from intra- to interspecific differentiation. Thus, combining different data types and species delimitation methods is needed to delineate species in this group.

Probably the most surprising result of these phylogenetic analyses is that, while the separate and combined mtDNA datasets consistently show a well-supported Trigoniulinae clade (based on three genera), they provide no support for the monophyly of the genus *Apeuthes*. This result corroborates the Trigoniulinae clade with two indicative, but not diagnostic, characters, viz (1) the presence of a mesal sternal process on the anterior gonopod and (2) a preanal ring without process protruding beyond the anal valves, i.e. two characters that are also present in most non-trigoniuline pachybolid genera. Conversely, the phylogenetic analyses cast some doubt on the monophyly of (the current concept of) the genus *Apeuthes* and thus question the defining synapomorphic nature of the posterior gonopod either with a boat-like cavity with several dentate, serrate or tuberculate lamellae or with a boat-like cavity covered with spines (Table 6). In conclusion, the assignment of the four new species, and particularly of ?*A. spininavis*, to the genus *Apeuthes* is provisional and must be validated by a

Table 6. Morphological differences between *Apeuthes*, *Eucarlia* and the four new species described in this study, viz *A. fimbriatus*, sp. nov., *Apeuthes longeligulatus*, sp. nov., *A. pollex*, sp. nov., and ?*A. spininavis*, sp. nov.

Characters	<i>Apeuthes</i>	<i>Eucarlia</i>	New species
A hook-like process on 5th coxae of male legs	–	√	–
Posterior gonopod telopodite with a sharp, pointed process	–	√	–
A flatten process on mesal margin at telopodite midway	–	√	–
Large tarsal pads on male legs	√	–	√
The part of the gonopod distal of the internal branch is longer than in 'the other (<i>Eucarlia</i>) species' and has several dentate, serrate or tuberculate lamellae in the boat-like cavity.	√	–	√ (in ? <i>A. spininavis</i> without the internal branch; but with a boat-like cavity covered with spines)

comprehensive integrative taxonomic and phylogenetic study involving a much wider sampling of taxa and phylogenetic DNA markers.

Supplementary material

Supplementary material is available [online](#).

References

- Attems CG (1909) Myriopoda. *Wissenschaftliche Ergebnisse der schwedischen Zoologischen Expedition nach den Kilimandjaro, dem Meru und den Umgebenden Massaiesteppen Deutsch-Ostafrikas 1905–1906* 19, 1–64.
- Attems CG (1914) Afrikanische Spirostreptiden nebst Überblick über die Spirostreptiden orbis terrarum. *Zoologica* 25(65–66), 1–235.
- Attems C (1938) Die von Dr C. Dawydoff in Französisch Indochina gesammelten Myriopoden. *Mémoires du Muséum national d'histoire naturelle, N.S* 6, 187–321.
- Attems CG (1953) Myriopoden von Indochina. Expedition von Dr C. Dawydoff (1938–1939). *Mémoires du Muséum national d'histoire naturelle, N. S., série A* 5(3), 133–230.
- Australian Society of Herpetologists (2016) Position statement #2 – taxonomy. Available at http://www.australiansocietyofherpetologists.org/s/ASH_Taxonomic_Position_Statement_Final-nrx5.pdf [Verified July 2021]
- Bickham JW, Parham JF, Philippen H-D, Rhodin AGJ, Bradley Shaffer H, Spinks PQ, van Dijk PP (2007) Turtle taxonomy: methodology, recommendations, and guidelines. *Chelonian Research Monographs* 4, 73–84.
- Bollman CH (1893) Classification of the Myriapoda. *Bulletin of the United States National Museum* 46, 153–162.
- Brandt JF (1833) Tentaminum quorundam monographicorum Insecta Myriapoda Chilognathi Latreillii spectantium prodromus. *Bulletin de la Société Impériale des Naturalistes de Moscou* 6, 194–209.
- Brölemann HW (1913) Un nouveau système de Spirobolides [Myriapoda, Diplopoda]. *Bulletin de la Société entomologique de France* 1913, 476–478.
- Butler AG (1876) Preliminary notice of new species of Arachnida and Myriapod from Rodriguez. *Annals and Magazine of Natural History, Series 4* 17, 439–446.
- Chamberlin RV (1921) V.—New Chilopoda and Diplopoda from the East Indian region. *Journal of Natural History Series* 97(37), 50–87. doi:10.1080/00222932108632489
- Cook OF (1897) New relatives of *Spiroboleus giganteus*. *Brandtia* 18, 73–75.
- Demange JM (1961) Matériaux pour servir à une révision des Harpagophoridae (Myriapodes-Diplopodes). *Mémoires du Muséum national d'histoire naturelle, N. S., Série A, Zoologie* 24, 1–274.
- Drummond AJ, Suchard MA, Xie D, Rambaut A (2012) Bayesian phylogenetics with BEAUti and the BEAST 1.7. *Molecular Biology and Evolution* 29, 1969–1973. doi:10.1093/molbev/mss075
- Edgar RC (2004) MUSCLE: multiple sequence alignment with high accuracy and high throughput. *Nucleic Acids Research* 32, 1792–1797. doi:10.1093/nar/gkh340
- Engelhof H (2011) East African giant millipedes of the tribe Pachybolini (Diplopoda, Spirobolida, Pachybolidae). *Zootaxa* 2753, 1–41. doi:10.11646/zootaxa.2753.1.1
- Engelhof H, Golovatch S, Short M, Stoev P, Wesener T (2015) Diplopoda – taxonomic overview. In 'The myriapoda 2. treatise on zoology – anatomy, taxonomy, biology'. (Ed A Minelli) pp. 363–453. (Brill: Leiden, Netherlands)
- Folmer O, Black M, Hoeh W, Lutz R, Vrijenhoek R (1994) DNA primers for amplification of mitochondrial cytochrome c oxidase subunit I from diverse metazoan invertebrates. *Molecular Marine Biology and Biotechnology* 3, 294–299.
- Fujisawa T, Barraclough TG (2013) Delimiting species using single-locus data and the generalized mixed Yule coalescent approach: a revised method and evaluation on simulated data sets. *Systematic Biology* 62, 707–724. doi:10.1093/sysbio/syt033
- Gervais P (1837) Etudes pour servir à l'histoire naturelle des Myriapodes. *Annales des Sciences naturelles, Série 2 Zoologie* 7, 35–60.
- Gervais P (1842) Myriapodes. *Voyage Autour du Monde exécuté pendant les années 1836 et 1837 sur la corvette La Bonite, commandée par M. Vaillant, Zoologie* 1, 276–280.
- Gervais P (1844) Etudes sur les Myriapodes. *Annales des Sciences naturelles, Série 3 Zoologie* 2, 51–80.
- Gervais P (1847) Myriapodes. In 'Histoire naturelle des Insectes'. (Ed. DA Walckenaer, P Gervais) Aptères 4, xvi + 333 (Roret: Paris, France)
- Golovatch SI, Korsós Z (1992) Diplopoda collected by the Soviet zoological expedition to the Seychelles Islands 1984. *Acta Zoologica Hungarica* 38, 1–31.
- Hillis D, Bull J (1993) An empirical test of bootstrapping as a method for assessing confidence in phylogenetic analysis. *Systematic Biology* 42, 182–192. doi:10.1093/sysbio/42.2.182
- Hoffman RL (1962) Studies on spiroboloid millipeds IV. Systematic and nomenclatorial notes on the family Pachybolidae. *Revue Suisse de Zoologie* 69, 759–783. doi:10.5962/bhl.part.75592
- Hoffman RL (1980) 'Classification of the diplopoda'. (Musée d'Histoire Naturelle de Genève: Geneva, Switzerland)
- Hoffman RL (1981) Studies on spiroboloid millipeds. XIV. Notes on the family Pseudospirobolellidae, and description of a new genus and species from Thailand. *Steenstrupia* 7(7), 181–190.
- Hoffman RL, Keeton WT (1960) A list of the generic names proposed in the diplopod order Spirobolida, with their type species. *Transactions of the American Entomological Society* 86, 1–26.
- Huelsenbeck JP, Ronquist F (2001) MrBAYES: Bayesian inference of phylogeny. *Bioinformatics* 17, 754–755. doi:10.1093/bioinformatics/17.8.754
- Jeckel CAW (2001) A bibliographic catalogue of the Spirobolida of the oriental and Australian regions (Diplopoda). *Myriapod Memoranda* 4, 3–104.
- Kaiser H, Crother BI, Kelly CMR, Luiselli L, O'Shea M, Ota H, Passos P, Schleip WD, Wüster W (2013) Best practices: in the 21st century, taxonomic decisions in herpetology are acceptable only when supported by a body of evidence and published via peer-review. *Herpetological Review* 44, 8–23.
- Karsch F (1881) Neue Juliden des Berliner Museums, als Prodromus einer Juliden-Monographie. *Zeitschrift für die gesammten Naturwissenschaften* 54, 1–79.
- Kessing B, Croom H, Martin A, McIntosh C, McMillan WO, Palumbi S (2004) PCR primers. In 'The simple fool's guide to PCR. Version 1.0'. (Eds S Palumbi, A Martin, S Romano, WO McMillan, L Stice, G Grabowski) pp. 17–18. (University of Hawaii, Department of Zoology: Honolulu, HI, USA)
- Kimura M (1980) A simple method for estimating evolutionary rates of base substitutions through comparative studies of nucleotide sequences. *Journal of Molecular Evolution* 16, 111–120. doi:10.1007/BF01731581
- Kumar S, Stecher G, Li M, Knyaz C, Tamura K (2018) MEGA X: molecular evolutionary genetics analysis across computing platforms. *Molecular Biology and Evolution* 35, 1547–1549. doi:10.1093/molbev/msy096
- Lanfear R, Frandsen PB, Wright AM, Senfeld T, Calcott B (2017) PartitionFinder 2: new methods for selecting partitioned models of evolution for molecular and morphological phylogenetic analyses. *Molecular Biology and Evolution* 34, 772–773.
- Mauriès JP, Engelhof H (1990) A new genus of cambaloid millipedes from Vietnam (Diplopoda: Spirostreptida: Cambalopsidae). *Entomologica Scandinavica* 21, 91–96.
- Miller MA, Pfeiffer W, and Schwartz T (2010) Creating the CIPRES Science Gateway for inference of large phylogenetic trees. In 'Proceedings of the Grid Computing Environments Workshop (GCE)'. 14 November 2010, New Orleans, LA, USA. INSPEC Accession Number: 11705685, pp. 1–8. (Institute of Electrical and Electronics Engineers: Piscataway, NJ, USA)
- Mwabvu T, Lamb J, Slotow R, Hamer RM, Barraclough D (2015) Do cytochrome c oxidase 1 gene sequences differentiate species of spirostreptid millipedes (Diplopoda: Spirostreptida: Spirostreptidae)? *African Invertebrates* 56, 651–661. doi:10.5733/afin.056.0311

- Pocock RI (1894) Contributions to our knowledge of the arthropod fauna of the West Indies. Part III. Diplopoda and Malacopoda, with a supplement on the Arachnida of the class Pedipalpi. *Journal of the Linnean Society of London* **24**(157), 473–519.
- Pimvichai P, Enghoff H, Panha S (2014) Molecular phylogeny of the *Thyropygus allevatus* group of giant millipedes and some closely related groups. *Molecular Phylogenetics and Evolution* **71**, 170–183. doi:10.1016/j.ympev.2013.11.006
- Pimvichai P, Enghoff H, Panha S, Backeljau T (2018) Morphological and mitochondrial DNA data reshuffle the taxonomy of the genera *Atopochetus* Attems, *Litostrophus* Chamberlin and *Tonkinbolus* Verhoeff (Diplopoda: Spirobolida: Pachybolidae), with descriptions of nine new species. *Invertebrate Systematics* **32**, 159–195. doi:10.1071/IS17052
- Pimvichai P, Enghoff H, Panha S, Backeljau T (2020) Integrative taxonomy of the new millipede genus *Coxobolellus*, gen. nov. (Diplopoda: Spirobolida: Pseudospirobolellidae), with descriptions of ten new species. *Invertebrate Systematics* **34**, 591–617. doi:10.1071/IS20031
- Puillandre N, Brouillet S, Achaz G (2021) ASAP: assemble species by automatic partitioning. *Molecular Ecology Resources* **21**, 609–620. doi:10.1111/1755-0998.13281
- Qu Z, Nong W, So WL, Barton-Owen T, Li Y, Leung TCN, Li C, Baril T, Wong AYP, Swale T, Chan TF, Hayward A, Ngai SM, Hui JHL (2020) Millipede genomes reveal unique adaptations during myriapod evolution. *PLoS Biology* **18**(9), e3000636. doi:10.1371/journal.pbio.3000636
- Rafinesque CS (1820) VI Class. Entomia. – the insects. *Annals of Nature* **1**, 7–10.
- Silvestri F (1897) Systema Diplopodum. *Annali del Museo civico di Storia naturale di Genova Serie 2* **18**, 644–651.
- Silvestri F (1909) Descrizione di una nuova famiglia di Diplopoda Cambaloidea del Tonchino. *Bollettino del Laboratorio di Zoologia generale e agraria della Reale Scuola superiore d'Agricoltura in Portici* **4**, 66–70.
- San Mauro D, Agorreta A (2010) Molecular systematics: a synthesis of the common methods and the state of knowledge. *Cellular & Molecular Biology Letters* **15**, 311–341. doi:10.2478/s11658-010-0010-8
- Stamatakis A (2014) RAxML version 8: a tool for phylogenetic analysis and post-analysis of large phylogenies. *Bioinformatics* **30**, 1312–1313. doi:10.1093/bioinformatics/btu033
- Tang CQ, Humphreys AM, Fontaneto D, Barraclough TG (2014) Effects of phylogenetic reconstruction method on the robustness of species delimitation using single-locus data. *Methods in Ecology and Evolution* **5**, 1086–1094. doi:10.1111/2041-210X.12246
- Vences M, Guayasamin JM, Miralles A, de la Riva I (2013) To name or not to name: criteria to promote economy of change in Linnaean classification schemes. *Zootaxa* **3636**, 201–244. doi:10.11646/zootaxa.3636.2.1
- Verhoeff KW (1938) Über Chorzognathen aus dem Zoologischen Museum in München. *Zoologischer Anzeiger* **124**, 303–320.
- Wesener T, Enghoff H (2009) Revision of the millipede subfamily Spiromiminae, a Malagasy group with Indian connections? (Diplopoda Spirobolida Pachybolidae). *Tropical Zoology* **22**, 71–120.
- Wesener T, Enghoff H, Hoffman RL, Wägele JW, Sierwald P (2009a) Revision of the endemic giant fire millipedes of Madagascar, genus *Aphistogoniulus* (Diplopoda: Spirobolida: Pachybolidae). *International Journal of Myriapodology* **2**(1), 15–52. doi:10.1163/187525409x462403
- Wesener T, Enghoff H, Sierwald P (2009b) Review of the Spirobolida on Madagascar, with descriptions of twelve new genera, including three genera of ‘fire millipedes’ (Diplopoda). *ZooKeys* **19**, 1–128. doi:10.3897/zookeys.19.221
- Xia X (2018) DAMBE7: new and improved tools for data analysis in molecular biology and evolution. *Molecular Biology and Evolution* **35**, 1550–1552. doi:10.1093/molbev/msy073
- Zhang J, Kapli P, Pavlidis P, Stamatakis A (2013) A general species delimitation method with applications to phylogenetic placements. *Bioinformatics* **29**(22), 2869–2876. doi:10.1093/bioinformatics/btt499

Data availability. The data that support this study are available in the article and accompanying online supplementary material or will be shared upon reasonable request to the corresponding author.

Conflicts of interest. The authors declare that they have no conflicts of interest

Declaration of funding. This research was funded by the Thailand Science Research and Innovation (TSRI) together with Mahasarakham University as a TRF Research Career Development Grant (2019–2022; RSA6280051) (to P. Pimvichai). Additional funding came from the Royal Belgian Institute of Natural Sciences (RBINS).

Acknowledgements. We thank Pongpun Prasankok for assistance in collecting material. We are indebted to Nesrine Akkari (NHMW) for providing specimens, Julien Cillis (RBINS) for help with SEM photographs, Yves Barette (RBINS) for help with gonopod photographs and to Thita Krutchuen (Chulalongkorn University) for the excellent drawings. We thank Henrik Enghoff (Natural History Museum of Denmark), Paul Marek (Virginia Polytechnic Institute and State University, USA) and Thomas Wesener (Zoological Research Museum Alexander Koenig, Bonn, Germany) for their critical comments and helpful discussions, which have substantially improved our manuscript.

Author affiliations

^ADepartment of Biology, Faculty of Science, Mahasarakham University, Maha Sarakham 44150, Thailand.

^BAnimal Systematics Research Unit, Department of Biology, Faculty of Science, Chulalongkorn University, Bangkok 10330, Thailand.

^CRoyal Belgian Institute of Natural Sciences, Vautierstraat 29, BE-1000 Brussels, Belgium.

^DEvolutionary Ecology Group, University of Antwerp, Universiteitsplein 1, BE-2610 Antwerp, Belgium.